

RESEARCH

Open Access



Experimental Study on Effect of Recycled Reinforced Concrete Waste on Mechanical Properties and Structural behaviour of the Sandy Soil

Ali Basha^{1*}, Fatma khalifa¹ and Sabry Fayed¹

Abstract

In recent years, constructing natural aggregates as a base layer for the roads has increased. Natural resources will run out as long as human consumption of them continues. Recycled concrete aggregate (RC) has thus emerged as a substitute material for the building of road base layers. Additionally, RC can be utilized to create interior city highways. The base layer for roads must have sufficient strength to support the working load on the pavement surface without damage deforming. As a result, the focus of this paper is on enhancing the structural performance of sandy soil reinforced with various RC percentages. The three key factors are relative soil density ($D_r = 83$ and 97%), recycled concrete aggregate reinforcing levels ($RC = 0, 5, 10, 15, 20, 25, 30, 40, 50$ and 100%), and reinforcement layer thickness ($R_d = 0.0B, 0.5B, B,$ and $2B$ where B is the footing model width). Numerous laboratory experiments were conducted in order to examine the impact of important parameters on the properties of the mixtures. The plate bearing tests were carried out using a footing model (250×250 mm) inside a tank ($1500 \times 1500 \times 1000$ mm) to ascertain the stress–strain response, bearing capacity ratio (BCR), ultimate bearing capacity, and modulus of elasticity of the tested mixtures. It is clear that raising the RC has no effect on the diameters of the grains. It was found that as RC increased, the mixture's bulk density increased but specific gravity decreased. Maximum dry density rose as RC rose, whereas water content fell. It was noted that BCR unquestionably increased as RC increased for all RC levels and all values of settlement ratios. The appropriate reinforcing layer thickness is suggested to be no more than $2B$. As the RC concentration in the sand and R_d increased, the difference between two pressure–settlement curves of densities 83% and 97% significantly decreased. Furthermore, when RC reaches 50% , two curves are roughly comparable. At $RC = 50\%$, it is advised that the relative density of 83% is sufficient to produce the same behavior as the relative density of 97% . It was found that as RC and R_d grew, the tested mixtures' ultimate bearing capacity and elasticity modulus increased as well. A novel proposed formulas are developed to compute bearing capacity ratio, ultimate bearing capacity, and elasticity modulus of the tested mixtures taking into account the influence of RC, reinforcement layer depth, settlement ratio, and the relative density, and its results agree with the experimental results.

Keywords Experimental study, Recycled concrete, Mechanical properties, Load-settlement behavior, Sandy soil, Bearing capacity, Highway base layer

Journal information: ISSN 1976-0485 / eISSN 2234-1315.

*Correspondence:

Ali Basha

ealibasha@eng.kfs.edu.eg

Full list of author information is available at the end of the article



© The Author(s) 2023. **Open Access** This article is licensed under a Creative Commons Attribution 4.0 International License, which permits use, sharing, adaptation, distribution and reproduction in any medium or format, as long as you give appropriate credit to the original author(s) and the source, provide a link to the Creative Commons licence, and indicate if changes were made. The images or other third party material in this article are included in the article's Creative Commons licence, unless indicated otherwise in a credit line to the material. If material is not included in the article's Creative Commons licence and your intended use is not permitted by statutory regulation or exceeds the permitted use, you will need to obtain permission directly from the copyright holder. To view a copy of this licence, visit <http://creativecommons.org/licenses/by/4.0/>.

1 Introduction

Large-scale production and use of building materials, as well as the resulting environmental contamination, have become a global issue. However, recycling garbage in infrastructure projects helps to counteract environmental damage while also maintaining the earth's natural resources. Because of the ongoing urbanization and population growth, the amount of acceptable soil accessible for civil engineering has become rather restricted. As a result, soil improvement has become mandatory in many conditions, including in situ soils, expenses, upkeep, and restricted soil (Al-Mukhtar et al., 2010; Latifi et al., 2014; Yong & Ouhadi, 2007). Soil improvement technologies are widely employed, particularly in soft and weak soils, pavements, foundations, or bituminous surface layers (Lim et al., 2021; Maghool et al., 2017; Mohammadinia et al., 2015). The use of natural resources in the foundation layer of roadways damages the natural resources, necessitating the search for new materials for the road layers. A well-designed roadway foundation layer would lessen the likelihood of asphalt stress cracking and ravelling.

Cement and lime are very well conventional soil enhancement binders (Ates, 2016; Mohammadinia et al., 2015). Soil particles exposed to these binders form chemical bonds between soil grains (Horpiulsuk et al. (2010), Blanck et al., 2014; Latifi et al., 2016; Shen et al., 2015). However, one significant drawback of cement is that it produces 6–8% of CO₂ (an important greenhouse gas produced by people) (Askarian et al., 2018; Pan et al., 2018). As a result, alternative binders have been thoroughly investigated in order to decrease the need of cement. As a result, rather than raising the cement ratio to achieve the required engineering qualities of soils, more cost-effective methods such as employing alternative materials such as building demolition wastes can be used. These wastes can be used to substitute cement or to reduce the cement ratio, allowing for more cost-effective and ecologically responsible alternatives.

Alkali-activated materials have recently emerged as a potential and sustainable alternative to conventional binders due to excellent technical qualities such as chemical resistance, fire resistance, sound absorption, cheap cost, environmental sensitivity, and fewer carbon emissions (Kim et al., 2013; Mohammadinia et al., 2019). A range of silica- and alumina-rich materials are added to alkali substances such as potassium hydroxide (KOH), sodium hydroxide (NaOH), calcium oxide, calcium hydroxide, potassium silicate, and sodium silicate (Islam et al., 2014; Maragos et al., 2009; Rowles & O'connor, 2003) in one alkali-activated approach.

Aluminate silicate is typically produced from furnace slags (Mohammadinia et al., 2018; Zhang et al., 2010),

fly ash (Zhang et al., 2014), red mud (Belmokhtar et al., 2017; V'asquez et al., 2016), metakaolins (Caballero et al., 2014), concrete demolition waste (Suksiripattanapong et al., 2017), mining wastes (Santa et al., 2013), rice husk ash (Vieira & Pereira, 2015), and calcined paper sludge (Zaetang et al., 2016). Construction demolition waste generally refers to numerous waste materials from civil engineering projects such as brick, concrete, wood, ceramics, plastic, bituminous mixes, glass, metals and soils (G'alvez-Martos et al., 2018). When RCAs are freshly crushed and conveniently watered, they present an improvement in their mechanical behavior and compressive strength. If it uses in road sub-base and it is treated correctly, freshly crushed and conveniently hydrated when it is spread and compacted, good results can be achieved. This will lead to a sustainable construction and a more resistant and durable structure (Jim'enez et al., 2012). Construction demolition debris accounts for around 35% of all garbage created in Europe, with the majority of it ending up in landfills (Ok et al., 2020). Almost all governments have begun to employ 70% of construction demolition trash in civil engineering projects, particularly in Europe and Turkey (Cristelo et al., 2013; Davies et al., 1999). There is a rising shortage of viable infrastructure development lands, specially roads. Lands with desirable geotechnical qualities are scarce and expensive. As a result, several soil stabilization procedures such as stabilization, grouting, and compaction are being examined in the development of soils in the aforementioned problematic locations in order to utilise them for building purposes. Nonetheless, the majority of the solutions suggested are expensive, time-consuming, and laborious.

Davies et al., 1999 investigated the impact of varying alkali-activated binder doses (20, 30, and 40%) on the characteristics of grout soil. According to Cristelo et al. (Rios et al., 2016), the possible fraction of activated fly ash for soft-soil stabilisation ranged from 20 to 40%. They discovered that a low calcium-based alkali activator with a dose range of 15 to 30% produced the best alkali efficiency of the fly ash for the enhancement of residual granitic soils. Pourakbar et al. (Arabani et al., 2013a) discovered that a geopolymer manufactured from agro-waste, palm oil fuel ash, and an alkaline solution including NaOH and KOH may be utilized to sustain soil strength gains. Rios et al. (Arabani et al., 2013a) produced geopolymer stabilization using a silty sand and alkaline activator solution to examine the applicability of geopolymer stabilization for small cost roads. They demonstrated that the road's strength and stiffness improved. (Pérez et al., 2012) confirmed that the replacement should not exceed 75% of RCAs in the case of light traffic for fear of permanent brain distortion. Arbain (Haider, et al., 2014) and Perez (Arulrajah et al.,

2013) suggest that the replacement rate in asphalt mixture should not exceed 60%.

As a result, millions of tons of graded natural aggregate are employed in the building of highway base layers pollute the environment and deplete natural sources. It is critical to discover a means to recycle the concrete waste materials, and roads offer a fantastic opportunity for this. Moreover, Concrete waste products are continually increasing as concrete building technology advances. These trashes will generate millions of tons of fill throughout the country over time. It is common knowledge that the utilization of old concrete debris to produce recycled concrete aggregate (RCA) has evolved into an innovative and viable alternative to natural aggregates. Concrete trash is one of the most prevalent waste products that stays in the environment for a long time, reducing the life of municipal disposal facilities if not repurposed. Additionally, RCA instead of virgin materials is more cost effective and decreases energy and virgin natural resource demands on the environment. To offer enough mechanical protection to the top pavement layers of the road pavement, loose coarse aggregates are widely employed in highway base or/and subbase constructions. Haider et al. (Cabalar et al., 2021).

In terms of geotechnical engineering properties in pavement subbases, RCA and waste rock were found to be equivalent to or superior to typical quarry granular subbase materials. (Ok et al., 2023). Evaluated the structural performance of RCA utilized in base layer of the highway roads. He investigated the engineering qualities of graded aggregate base course material, RCA, and combinations of the two. He also investigated the effect of curing duration and winter circumstances on RCAs. The results revealed that RCA had better engineering qualities than conventional graded aggregate base course due to the presence of more CaO in the soil matrix, which begins the cementitious reaction and improves mechanical capabilities. The testing analysis indicate that the construction demolition materials increased the ultimate bearing capacity of the clay by 50–75%. (Mehrjardi et al., 2020). Although it was noted that construction demolition performed worse than virgin aggregate, it was determined that construction demolition performed well enough to be used as an alternative to virgin aggregate on roadways. Furthermore, it was determined that the construction demolition could perform better virgin aggregate with a very small number of geosynthetics (Geckil et al., 2022). The result indicated that the physical and mechanical properties of the construction demolition materials studied agreed with the majority of the standard criteria to be utilized as sub-base materials in road construction (ECP-202, 2018).

Soil stabilization goals to raise shear capacity, reduce permeability, and boost hardness and uniformity in coarse and fine-grained soil properties. Soil treatment and stabilization, in general terms, refers to a variety of treatments designed to enhance the mechanical behaviour of soils and lower building costs. The use of wastes in soil improvement operations done using geotechnical technologies has grown increasingly widespread. As a result, significant benefits of using wastes in such procedures include reducing the amount of cumulative waste in the environment, lowering storage costs and related taxes, and implementing wastes to improve existing soil conditions rather than using expensive additives or at least lowering the amounts of such additives. By constructing one of the CDW or NA fillings on the weak soil, the bearing capacity and settlement could be increased. It is possible to make sure that the applied stress is carried by the stiffer soil layer and that the stress coming to the weak soil is reduced by constructing a stiffer soil layer on the weak soil (ASTM D, 2487 Standard Practice for Classification of Soils for Engineering Purposes 2017).

Although various concrete technology applications demonstrating that the alkali/cement ratio is critical in determining target strength, there is a substantial paucity of study on the efficacy of large-scale soil enhancements dependent on recycled concrete. As a result, this study is focusing on behaviour improvement of the sandy soil utilizing recycled concrete aggregate (RCA) as a reinforcing material. Several laboratory experiments were performed on RCA-sand mixtures at replacement levels (0, 5, 10, 15, 20, 25, 30, 40 and 50%). The main parameters are RCA content (RC), reinforcement layer thickness (R_d), relative density (D_r). In addition, mechanical properties and structural performance of unreinforced and reinforced sandy soil were performed in terms of physical characteristics, maximum dry density, optimum water content, contact stress -settlement relationships, bearing capacity ratio (BCR), ultimate bearing capacity (q_u), modulus of elasticity (E). Further, new proposed formulas are derived to estimate q_u and E of RC-reinforced soil. Additionally, a statistical study depending on the current results is performed for future evaluation of ultimate bearing capacity (q_u), modulus of elasticity (E) of RC-reinforced soil.

2 Materials

2.1 Pure Sand

The sand utilized in this investigation is river sand from a nearby river. The sieve analysis experiments are used to determine the physical qualities of the sand, as illustrated in Fig. 1. The sand index characteristics will determine in following sections with other tested mixtures. The sand is classified as poorly graded according to Egyptian code ECP-202 (2018) (Basha, 2021). In addition, according to

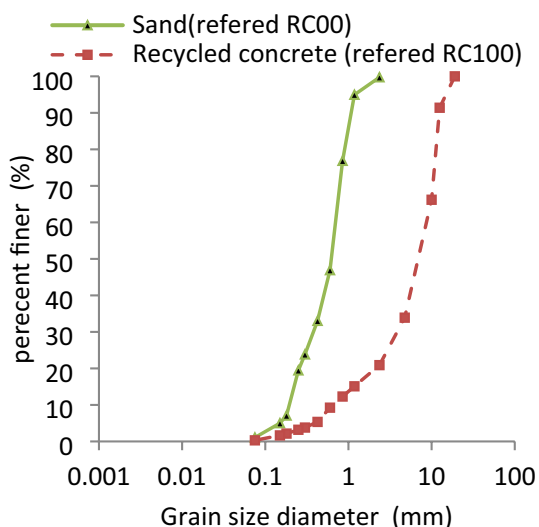


Fig. 1 Grain size distribution curves of the recycled concrete (RC) and unreinforced (pure) sand (US), RC is labeled RC100 and US is denoted by RC00

ASTM D 2487 (Kim & Jeong, 2011), US is categorized as uniform clean sand and its particles are defined as medium to coarse particles. The specific gravity of US is estimated as 2.5 (Basha, 2021). US composed of 95% SiO₂ and 2% Al₂O₃ (according to results of X-rays).

2.2 Recycled Concrete (RC)

The recycled concrete (RC) used in this study was created by reusing discarded reinforced concrete beams (Fig. 2a) The mean compressive strength of concrete core samples taken from the beams used in the study was 30 MPa. The RCs were prepared in two stages. The first stage was hand crushing of reinforced concrete beam debris into small pieces up to 150 mm in size, followed by rebar extraction

(Fig. 2b). The second step used mechanical crushing using an electromechanical crushing machine (Fig. 2c). The crusher output regulated the RC grading. The RC particle size ranges from 0.075 to 19 mm as a result (Fig. 1). The size of the RC is chosen to be more realistic and similar to graded natural aggregate used in the construction of roadway base layers. The sieve analysis test was used to determine the grain size distribution of RC, which is depicted in Fig. 1. The designations and features of RC will summarize in in following sections with other tested mixtures. According to Egyptian code ECP-202 (Basha, 2021), the RC utilized is of good quality of grading. The RC utilized has a specific gravity of 2.5. After the final stage, sieve No. 200 (opening size 0.075 mm) is used to separate the fine materials, then the RC were washed and submerged in water for 24 h, then dried in the air for at least 76 h before using it in conducting tests. RC composed of 60% CaO, 9% Al₂O₃ and 20% SiO₂ so that RC is a strong candidate for employ as a soil stabilizer in alkaline activation techniques.

3 Methodology

The experiments were conducted on rigid steel plate which has dimensions of 250×250 mm and had a thickness of 50 mm. This plate is simulating a square footing model with width B=250 mm. The applied load is centrally acted on the center of the plate which placed on the surface of tested soil sample. The soil mixture was casted inside a rigid box steel tank (Fig. 3). The tank walls and base consisted of metal plates with 5 mm thickness strengthened by outer horizontal stiffeners so that lateral deformation of the tank sides is prevented during testing.

The tank’s internal dimensions were chosen to eliminate the boundary effect. It is important to remember that friction between the soil and the tank wall can cause the vertical stress in the soil to be reduced. The



Fig. 2 Production steps of RC

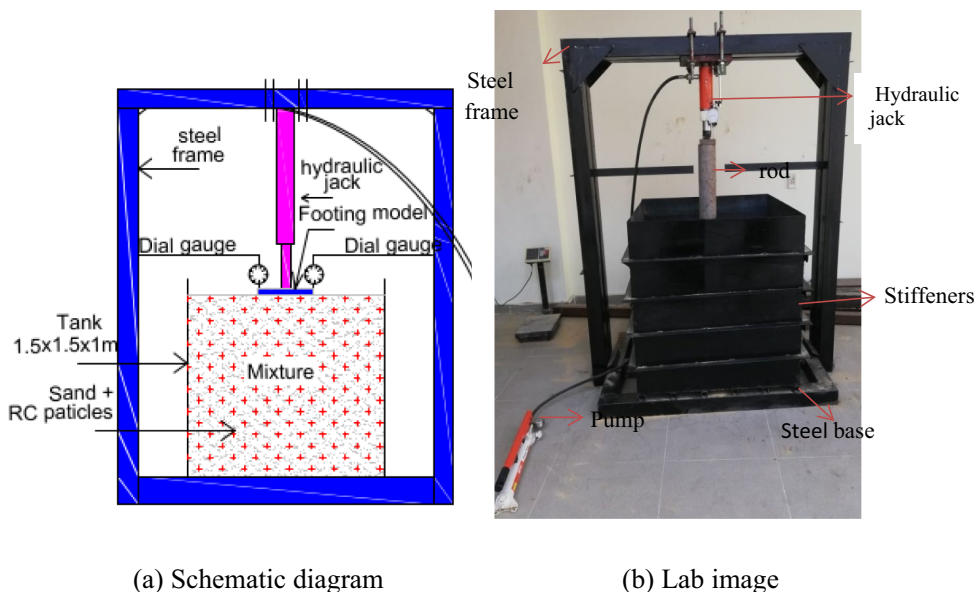


Fig. 3 Testing setup

inside wall of the tank was smoothed out to reduce friction with the soil as much as possible to reduce such an interaction. Basha (IS, 1983) investigated an experimental study on the piles inside a tank and the results showed that the area of the soil affected by the tank boundaries varies depending on the pile installation method and the relative density of the soil. According to Kim and Jeong (Gill & Mittal, 2019), to avoid the boundary effect, the tank’s diameter dimension be at least 11 times the pile’s diameter. Also, according to Basha (IS, 1983), the zone of impact for the piles is 3–8 times the diameter of the pile. Based on these studies, tank width-footing width ratio was selected as 6 to avoid boundary condition effects. Tank size is 1.5 m in width, 1.5 m in length and 1 m in height. To apply the load, a hydraulic jack with capacity of 25 ton is installed at the top of the steel frame. Hydraulic jack and footing model are justed at the middle of the tank. To simulate the actual conditions of the footing loading, a very slow loading rate was performed (loading rate = 8 kN/m² per min). After filling tested sand mixture, footing model is placed at the tank center then its horizontal level is well adjusted to avoid any tilt. After that, two displacement dial gauges (sensitivity = 0.01 mm) are used to measure settlement of footing model. Then, the average of two dial gauges was obtained. The tank is filled with 8 equal depth layers after the tested soil mixture manufacture. Each layer’s required weight is inserted at a given depth using manual compacting to achieve relative density $D_r = 83%$ or $D_r = 97%$. Because of the large fluctuation in the size of RC and its high hardness, the

quantity of compacting effort was raised as the quantity of RC in the mixture was elevated to obtain the required density.

In two situations ($D_r = 83%$ and $D_r = 97%$), the requisite weights of US and RC for each sample were estimated for sand mixture manufacturing. The low D_r of 83% was chosen to be more realistic and comparable to the good compaction level (designated as dense) of graded natural aggregate used in the building of rural road foundation layers. A high D_r of 97% was chosen to be comparable to the entire compaction level (designated as extremely dense) of graded natural aggregate used in the building of urban road foundation layers. According to IS-2720 Part 14 (Ladd, 1978), laboratory tests are performed on US to obtain maximum and minimum dry density corresponding to relative densities of 83% and 97% which obtained as 1.8 and 1.85 gm/cc. For each layer, to remain density of the mixture at 1.8 or 1.85 gm/cc, Eq. (1) was used to estimate required mass of RC and US.

$$\rho = \frac{M_{US} + M_{RC}}{V} \tag{1}$$

where, M_{US} is mass of the unreinforced sand (US), M_{RC} is mass of the recycled concrete (RC) and V is volume of the one layer of the tank which equal width × length × specific depth. After preparation of required weights, the mixture is well manually mixed until there is homogeneity in the RC distribution within the sand. This procedure is similar one that conducted in ASTM (1978); (Harr, 1966). Moreover, the approach used in this research is straightforward and similar to that used in the field.

Table 1 contains information on all of the soil combinations that were tested. This research focuses on improving the behaviour of sandy soil by employing recycled concrete (RC) as a reinforcing element. On RC-sand mixtures, eighteen laboratory tests were carried out at different replacement amounts (0, 5, 10, 15, 20, 25, 30, 40, and 50%). The major factors are the RC content, the thickness of the reinforcing layer (R_d), and the relative density (Dr). R_d is varying which equal 0, 0.5, 1, 2 and 4 times the width of the footing (B). also, two Dr (83% and 97%) are carried out.

4 Effect of RC Content on Soil Characterization

Each sample is individually prepared by bring required weight of the recycled concrete (RC) as well as required weight of the pure sand. After that, these weights were put on a completely clean wooden board and then stir well until homogeneity took placed. After that, the tank was filled in separate layers to adjust the determined density. As shown in Table 1, eighteen tests were carried out in the tank, but only 9 mixes were investigated in this research, including one unreinforced pure sand (US83 and US97, which were merely sand but with two different compaction levels) and 8 reinforced by RC (RC05-83, RC10-83, RC15-83, RC20-83, RC25-83, RC30-83, RC40-83, RC50-83). In other words, the rested tested samples

are similar with these nine samples except relative density of thickness of reinforcement layer. For simplifying, these nine mixtures (US83 or US97, RC05-83, RC10-83, RC15-83, RC20-83, RC25-83, RC30-83, RC40-83, RC50-83) may be labelled as RC00, RC05, RC10, RC15, RC20, RC25, RC30, RC40, RC50. Where the first two letters (RC) denote recycled concrete and the next two numerals reflect the RC replacement level. It should be noted that mix RC00 is the same as mixture US (pure sand), the grading curves of which are shown in Fig. 1. Also, the RC sample shown in Fig. 1 is a mixture comprising 100% RC, hence it is indicated as RC100 in this section. In each experiment, a specified weight (50 kg) was extracted from the mixture during tank filling to perform sieve analysis, compaction modified proctor, and other tests according to Egyptian code ECP-202 (Basha, 2021).

4.1 Sieve Analysis Test

Fig. 4 shows grain size distribution relationships of eight tested mixtures from RC05 to RC50 while grain size distribution curves of two tested mixtures RC00 and RC100 are drawn in Fig. 1. To evaluate mixing process quality of each mixture, theoretical grain size distribution curve was calculated and drawn in the figure of the same mixture. Grain size of two samples (RC00 and RC100) shown in Fig. 1, was used to predicted theoretical grain

Table 1 Details of tested soil mixtures

| Test series | Experiment no | Mixture ID | RC (%) | Dr (%) | R_d | No. of tests | |
|------------------|---------------|--------------|--------|--------|---------------------------|--------------|------|
| Effect of RC | 1 | US83 | 0 | 83 | 0 | 9 | |
| | 2 | RC05-83 | 5 | | Full depth of the tank=4B | | |
| | 3 | RC10-83 | 10 | | | | |
| | 4 | RC15-83 | 15 | | | | |
| | 5 | RC20-83 | 20 | | | | |
| | 6 | RC25-83 | 25 | | | | |
| | 7 | RC30-83 | 30 | | | | |
| | 8 | RC40-83 | 40 | | | | |
| | 9 | RC50-83 | 50 | | | | |
| | 10 | US97 | 0 | 97 | Full depth of the tank=4B | 3 | |
| 11 | RC25-97 | 25 | | | | | |
| 12 | RC50-97 | 50 | | | | | |
| Effect of R_d | 13 | RC25-83-0.5B | 25 | 83 | 0.5B | 6 | |
| | 14 | RC25-83-B | | | B | | |
| | 15 | RC25-83-2B | | | 2B | | |
| | 16 | RC25-97-0.5B | | | 97 | | 0.5B |
| | 17 | RC25-97-B | | | | | B |
| | 18 | RC25-97-2B | | | | | 2B |
| Effect of $Dr\%$ | 1 | US83 RC00-83 | 0 | 83 | | 0 | - |
| | 10 | US97 RC00-97 | 0 | 97 | 0 | | |
| Total tests | | | | | | 18 | |

RC is recycled concrete reinforced soil mixture, Dr is relative density of the mixture, R_d is reinforcement depth and B is footing model width

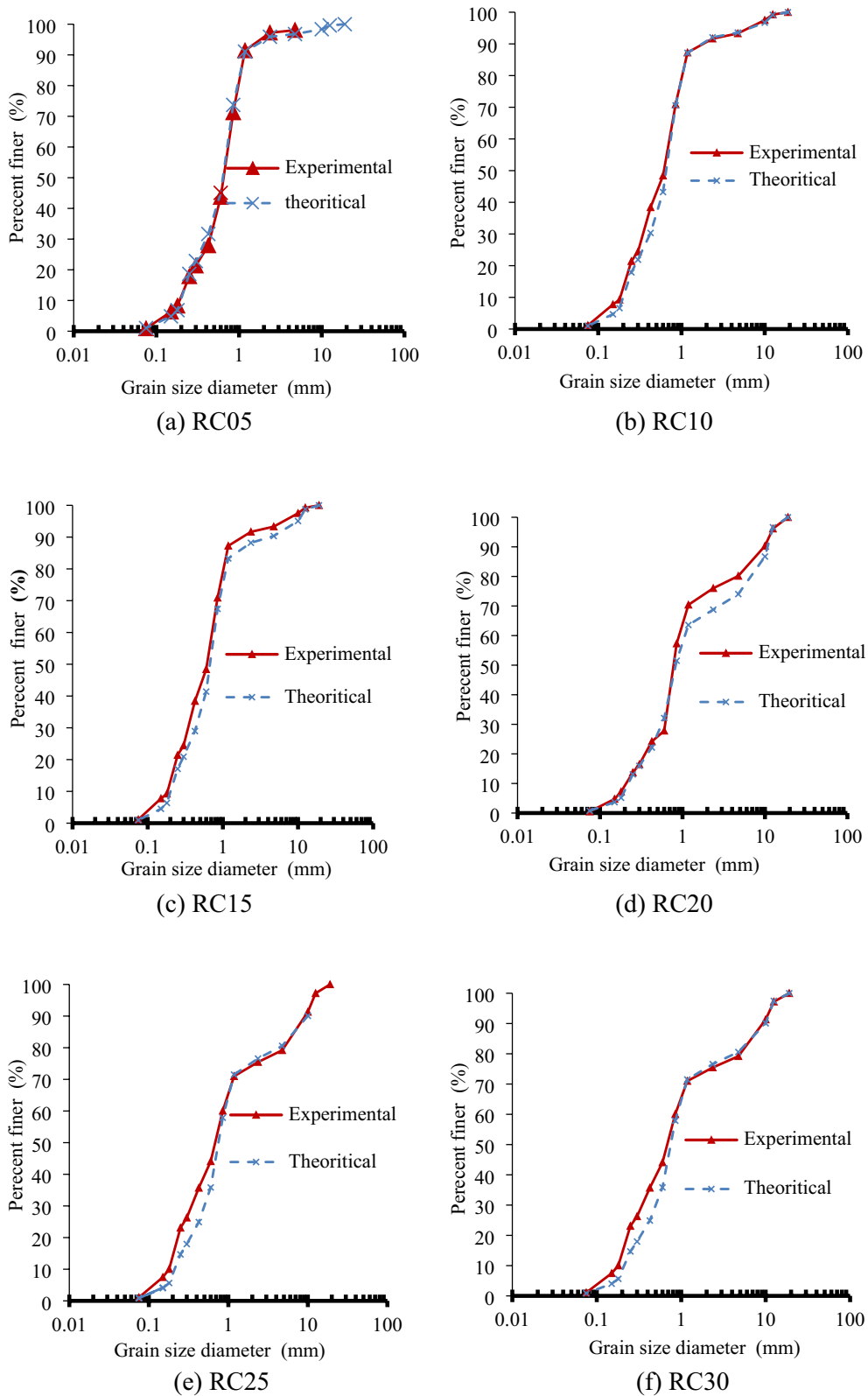


Fig. 4 Experimental and theoretical grain size distribution curves of tested samples

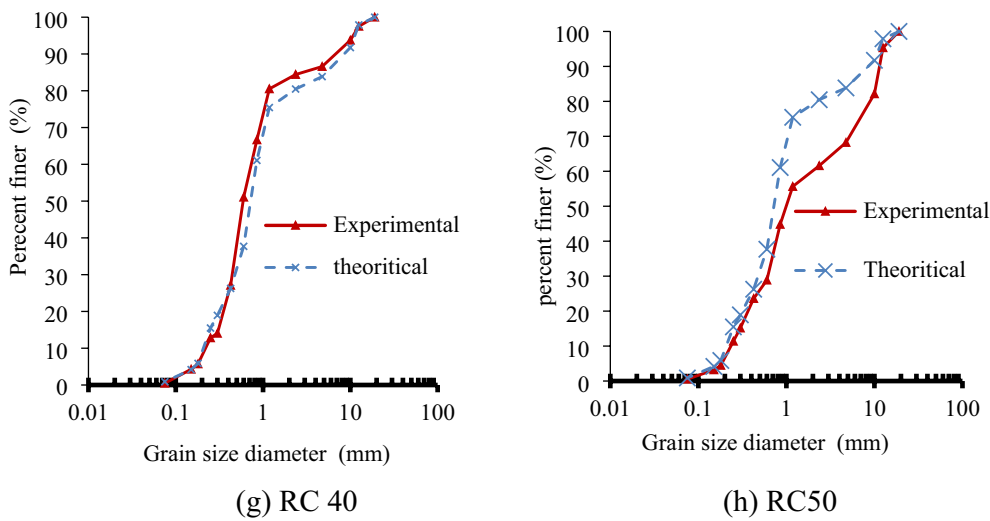


Fig. 4 continued

size distribution curve of each mixture. Values of Percent finer (vertical axes) related to grain size diameter values were obtained for RC00 and RC100. The Percent finer values of each mixture were then computed by multiplying the RC and sand percentages by the percent finer of RC100 and RC00, respectively. For example, the RC and sand percentages in RC25mixture are 0.25 and 0.75, respectively. When experimental grain size curves are compared to theoretical ones, the experimental findings are quite near, proving that the given technique for mixing the RC inside the sand is good and valid in field application.

Effective grain size (D_{10}) and average grain size (D_{50} and D_{60}) are obtained from grain size curves. Additionally, uniformity coefficient (C_u), coefficient of curvature (C_c) and are estimated using equations of ECP202 (Basha, 2021). Bulk density (BD) and specific gravity (G_s) of all mixtures is experimentally found. Maximum dry density (MDD) and

optimum water content (OMC) were determined. All these results are listed in Table 2.

Relations between RC percentage and grain size diameters of tested mixtures It is clear that raising the RC up to 40% has no effect on the grain size diameters, and increasing it from 40 to 50% has only a little effect on the diameters. When the RC surpasses 50%, the rate of rise in diameters is quite rapid. Because of the increasing grain size of the mixes, this effect is rational and predicted.

Uniformity coefficient (C_u), coefficient of curvature (C_c) are estimated using following equations:

$$C_u = \frac{D_{60}}{D_{10}} \tag{2}$$

$$C_c = \frac{D_{30}^2}{D_{10}D_{60}} \tag{3}$$

Table 2 Properties of tested mixtures

| Sample | D_{10} (mm) | D_{50} (mm) | D_{60} (mm) | C_u | C_c | G_s | BD (kN/m ³) | MDD (kN/m ³) | OMC (%) |
|--------|---------------|---------------|---------------|-------|-------|-------|-------------------------|--------------------------|---------|
| RC00 | 0.22 | 0.62 | 0.700 | 3.19 | 2.2 | 2.67 | 14.4 | 18.6 | 16 |
| RC05 | 0.1926 | 0.6574 | 0.7481 | 3.5 | 1.9 | 2.65 | 14.55 | 18.7 | 15.6 |
| RC10 | 0.195 | 0.6177 | 0.728 | 3.7 | 1.5 | 2.63 | 14.6 | 19.1 | 15.1 |
| RC15 | 0.222 | 0.6398 | 0.7744 | 3.8 | 1 | 2.62 | 14.75 | 19.1 | 14.3 |
| RC20 | 0.232 | 0.6412 | 0.75 | 3.9 | 0.6 | 2.61 | 14.8 | 19.6 | 13.9 |
| RC25 | 0.222 | 0.592 | 0.7435 | 3.95 | 0.5 | 2.58 | 14.95 | 20 | 13.5 |
| RC30 | 0.24 | 0.6926 | 0.8493 | 4 | 0.4 | 2.57 | 15 | 20.5 | 12.9 |
| RC40 | 0.222 | 0.6398 | 0.7744 | 4.2 | 0.38 | 2.54 | 15.3 | 20.7 | 12.4 |
| RC50 | 0.236 | 1.008 | 1.230 | 4.3 | 0.36 | 2.52 | 15.5 | 20.9 | 12.1 |
| RC100 | 0.63 | 7.36 | 8.990 | 14 | 0.16 | 2.5 | 14.05 | 21 | 9.5 |

for all tested samples. Due to D_{60} increased with rise of RC content, uniformity coefficient (C_u) slowly increased when RC increased from 0 to 50%. But when RC reached 100%, C_u clearly increased due to absence fine particles of the sand in this mixture (RC100). On contrast, C_c declined as RC increased because the C_c is inversely proportional to the diameter D_{60} which increased as RC rose.

4.2 Bulk Density and Specific Gravity Test

Laboratory tests for determining bulk density (BD) and specific gravity (G_s) are performed on all tested mixtures. The pycnometer was used to determine the specific gravity. RC contents were drawn against BD and G_s , as shown in Fig. 5. It was seen that as RC increased up to 50%, BD increased. Because the weight of the RC particles is greater than that of sand particles and with increase of RC in the mix, RC particles increased. due to absence sand fine particles in completely RC mixture (RC100), BD declined at RC increased more than 50%. As illustrated in Fig. 5b, it was seen that as RC increased, G_s declined as expected due to increasing voids as RC increased.

4.3 Compaction Modified Proctor Test

Compaction is the process of decreasing voids in soil to enhance density. The purpose of this test is to identify the soil's maximum dry density (MDD) and optimal moisture content (OMC). Soils having a low OMC and a large MDD can be useful in many engineering applications, particularly in road foundation layer and replacement layer under the building foundation. The compaction tests were conducted to evaluate OMC and MDD for

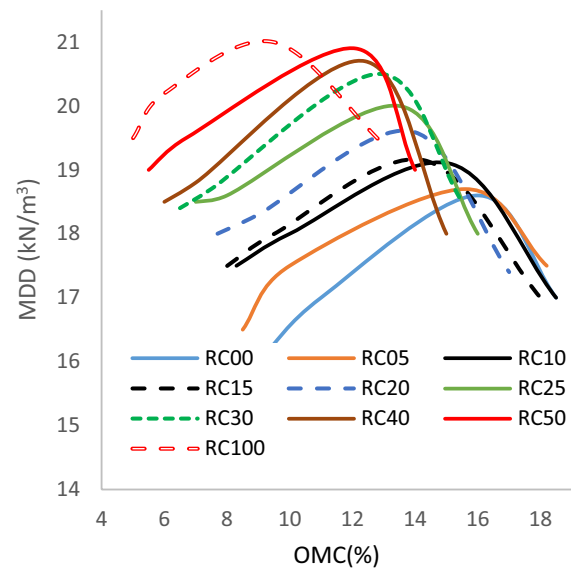
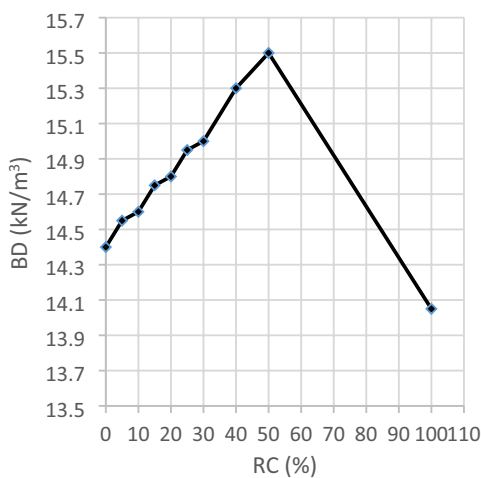
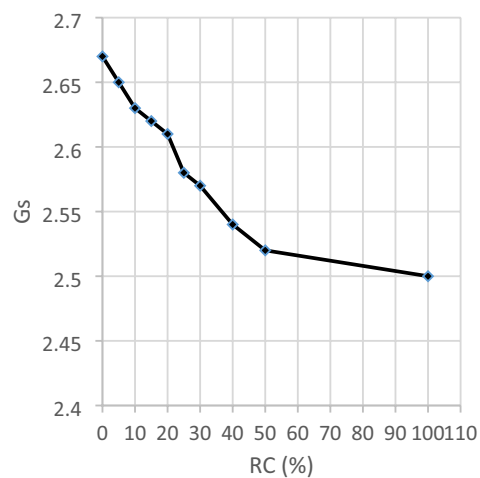


Fig. 6 Compaction curves for all presented mixes incorporating different levels of RC

all presented mixes. Fig. 6 shows the compaction curves for all presented mixes incorporating different levels of RC. RC content was drawn versus OMC and MDD, as illustrated in Fig. 7. It was discovered that when RC increased, OMC decreased. This might be because when the RC in the mix grew, the number of particles reduced, resulting in a decrease in the surface area of the particles and, as a result, the needed water quantity for granule surface coating. This resulted in compaction with very little water. As required water quantity for reaching MDD



(a) BD



(b) G_s

Fig. 5 RC content vs BD and G_s for all tested samples

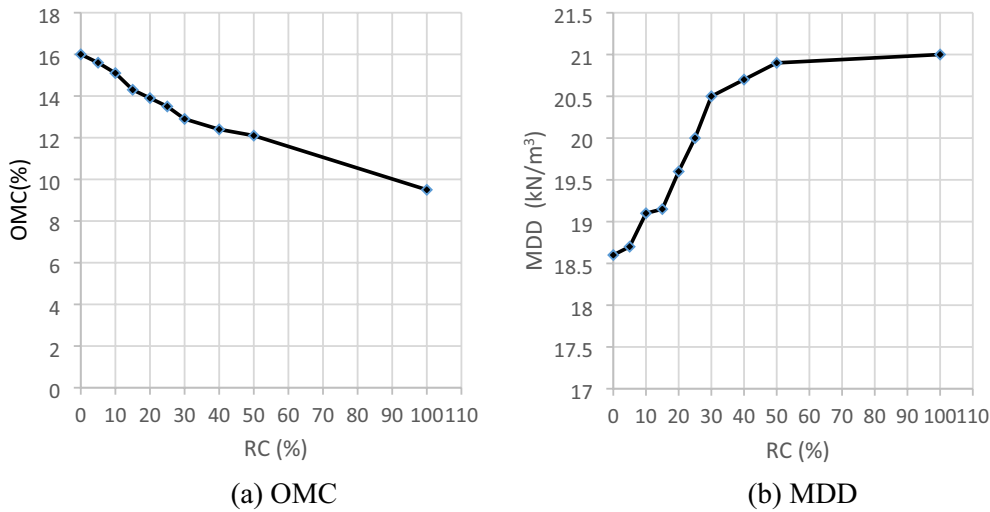


Fig. 7 RC content vs OMC and MDD for all tested samples

declined, the cost and time of the project will decrease. When seen in Fig. 9b, as RC rose, MDD improved significantly. This occurred because as the RC increased, the particle weight of the mixture increased and sand filled the spaces of the RC particles, resulting in a decrease in porosity and voids and an increase in the weight and density of the mix. As a result, RC had a substantial influence on enhancing soil OMC and MDD, and it is a suitable choice for creating road foundation layers or as replacement material to decrease the foundation depth. High MDD is required in the building of road foundation layers to prevent deformability of the surface layer (asphalt) under traffic stresses.

5 Results and Discussion

A total of 18 experiments were carried out on unreinforced sands (RC00) and RC-mixes at two D_r (83% and 97%). Load-settlement relationship was obtained for each mixture using plate bearing tests which performed in the tank. Load converted to load intensity (stress) and settlement (s) converted to settlement ratio (s/B) to be more realistic and valid for field application and for future additional investigations. The applied load was divided by area of the footing model (plate area) to calculate load intensity (stress), and B is the plate width. From stress-s/B curve of each sample, carrying bearing capacity was determined at different values of s/B for estimating normalized bearing capacity ratio (BCR) which is calculated as below:

$$BCR = \frac{\text{Bearing capacity of RC mixture}}{\text{Bearing capacity of pure sand mixture}} \quad (4)$$

where bearing capacity referred to the load intensity at specific value of s/B. This section will discuss effect recycle concrete waste percentage (RC), reinforcement layer thickness (R_d) and relative density (D_r) on stress-settlement ratio response and BCR (Sect. 5.1). While Sect. 5.2 will explain effect of key parameters on modulus of elasticity and ultimate bearing capacity of the soil.

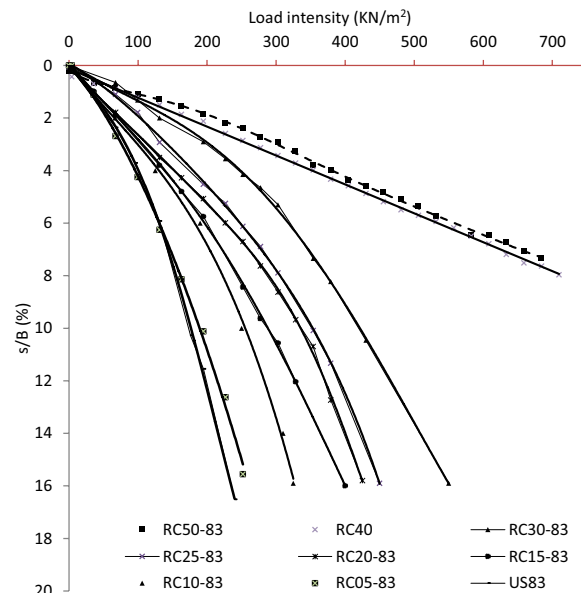


Fig. 8 Load settlement curves of mixtures at different RC ($D_r = 83\%$)

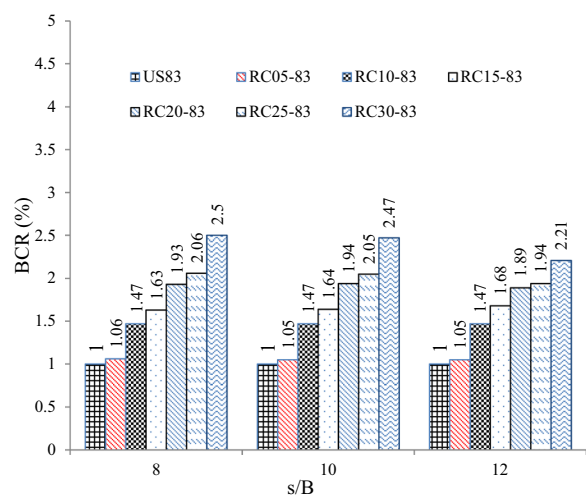


Fig. 9 Impact of RC on BCR at varied s/B (Dr = 83%, R_d = 4B)

5.1 Load-Settlement Response

5.1.1 Influences of RC

5.1.1.1 Dr=83% For the mixtures that compacted at Dr=83%, the load intensity-s/B relationships were drawn in Fig. 8. In general, as load intensity increased, the s/B increased until test end, all sample behaviour follow the general shear failure mode. At the beginning of the loading, it is noted that the curves are identical for all samples. All mixtures behaved a nonlinear relationship except two mixtures RC40-83 and RC50-83 which had linear behavior from beginning to finishing the loading. It is well known that as the soil carried more stress at small level of settlement (s/B), this demonstrating it had a good structural performance under the loading. So that, it was seen that using RC as a reinforcement material inside the soil significantly improved stress-settlement relationship. Moreover, as RC increased, the soil achieved a higher stress-settlement relationship until RC of 40 and 50% could convert the weaken nonlinear stress-settlement relationship into strong linear one (specimen RC40-83 and RC50-83). In the other words, energy capacity (area under the curve) remarkably increased with increase of RC. This took placed due to high bearing resistance of the RC particles which is higher than the sand particles. Also, big variation in particles size of RC and sand clearly declined the porosity hence increase the density hence the bearing capacity increased gradually as RC particles increased within the mixture. Two curves of specimens US83 and RC05-83 are approximately close due to low RC (5%) did not can improve the mechanical behavior of the

soil. On contrast, using 50% RC caused a remarkable effect on the bearing capacity at all different levels of settlement. It is well known that as the reinforcement material quantity increased, the road base layer building will raise. It was shown that when RC increased over 40%, the stress-settlement relationship did not influence, demonstrating that the optimum RC content is 40% at Dr=83%. Unlike samples RC40-83 and RC50-83, any minor increase in stress above 150 kN/m² generates a fast rise in settlement for mixtures reinforced with a low quantity of RC. It was discovered that the value 150 kN/m² is around half of the reinforced soil's final bearing capability. Furthermore, this value 150 kN/m² is close to the acceptable bearing capacity specified by ECP 202 (Basha, 2021).

To understand effect of RC on load carrying capacity stress of the soil, amount of RC in the mixtures was varied from 0 to 50%. Also, load carrying capacity was studied at settlement ratio (s/B) equal 2, 4, 6, 8, 10 and 12%. The increase in the bearing resistance of the mixture was estimated using BCR. Change in BCR at different s/B (%) is illustrated in Fig. 9 for specimens that compacted at Dr=83%. It was seen that as RC increased, BCR clearly enhanced for all RC levels (0–50%) at all values of s/B (2 to 12%). BCR obtained at s/B=2% for RC 5, 10, 15, 20, 25, 30, 40 and 50% was 1.2, 1.5, 1.6, 1.7, 2.2, 3, 4 and 4.6. Also, BCR obtained at s/B=4% for RC 5, 10, 15, 20, 25, 30, 40 and 50% was 1.11, 1.39, 1.44, 1.67, 2, 2.56, 2.78 and 4. Additionally, BCR obtained at s/B=6% for RC 5, 10, 15, 20, 25, and 30 was 1.04, 1.44, 1.52, 1.76, 2 and 2.56. BCR obtained at s/B=12% for RC 5, 10, 15, 20, 25, 30, 40 and 50% was 1.05, 1.47, 1.68, 1.89, 1.94 and 2.21. Because the permitted settlements for foundations on fine-grained soils (i.e. sandy soil) are not particularly large, the behavior at low strains (s/B=2, 4 and 6%) is crucial from a design standpoint. It was discovered that the increase in BCR was greatest at very small strains (s/B=2%) and least at very big strains (s/B=12%) where the BCR reach about 4 and 4.60 for RC40-80 and RC50-83 respectively at s/B=2%. Furthermore, when the amount of strain increased, the rise in BCR decreased. As a result, utilizing RC as a reinforcing material in granular soil (sand) is a great and beneficial design choice due to the substantial increase in bearing capacity at low settlement.

5.1.1.2 Dr=97% For the mixtures that compacted at Dr=97%, stress-s/B relationships were drawn in Fig. 10. In general, as load intensity increased, the s/B increased until test end. Approximately, all mixtures with Dr=97% behaved a linear relationship unlike mixtures with Dr=83 which exhibited a nonlinear curve due to its high den-

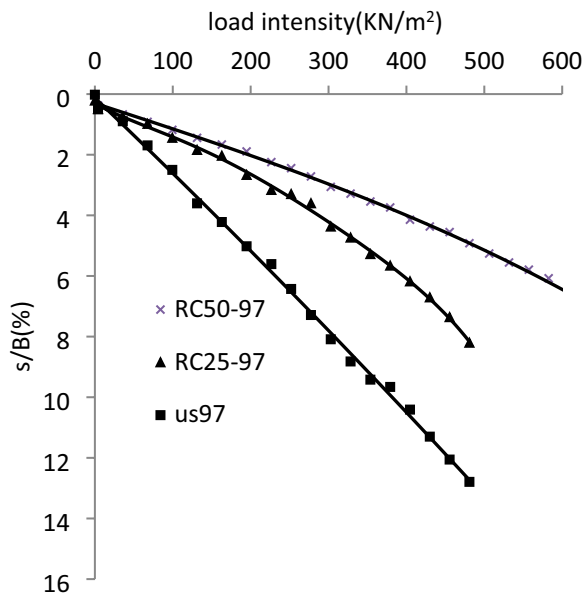


Fig. 10 Load settlement curves of mixtures at different RC (Dr=97%)

sity demonstrating that the well compacted soil achieved better behavior than medium compacted soil. When reinforced mixtures (RC25-97 and RC50-97) compared to unreinforced sample (US97), it was seen that using RC as a reinforcement material inside the soil significantly improved stress-settlement relationship. In the other words, energy capacity remarkably increased with increase of RC due to same reasons mentioned before.

To determine whether the effect of RC content on the carrying capacity stress of the mixtures at Dr=97% is

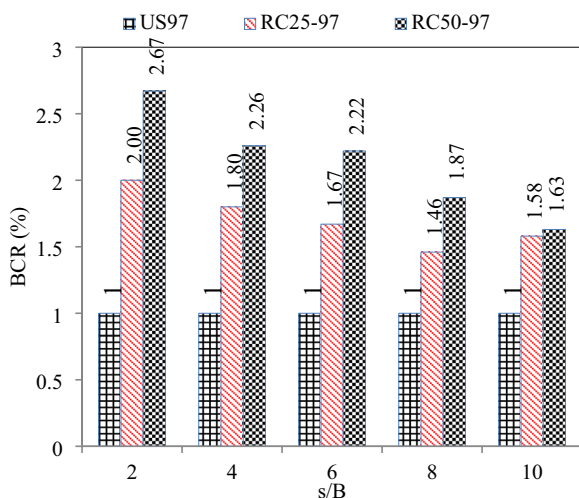


Fig. 11 Impact of RC on BCR at varied s/B (Dr = 97%, $R_d = 4B$)

beneficial and comparable to the mixtures at Dr=83%, two RC contents (25 and 50%) were assessed in the mixtures RC25-97 and RC50-97. Load carrying capacity was also investigated at settlement ratios (s/B) of 2, 4, 6, 8, and 10%. Fig. 11 depicts the change in BCR at various s/B (%) for specimens RC25-97 and RC50-97 in comparison to control specimen US97. BCR obviously rose when RC climbed from 25 to 50% at all s/B levels (2–10%). The BCR obtained at s/B=2% for RC 25 and 50% was 2 and 2.67, respectively. Furthermore, the BCR achieved at s/B=4% for RC 25 and 50% was 1.8 and 2.26, respectively. Furthermore, the BCR measured at s/B=6% for RC 25 and 50% was 1.67 and 2.22, respectively. The BCR achieved at s/B=10% for RC 25 and 50% was 1.58 and 1.63, respectively. As with the Dr 83% mixes, it was determined that the rise in BCR was highest at small strains (s/B=2%) and least at large strains (s/B=10%). Furthermore, when the degree of strain grew, so did the rise in BCR. As a result, using RC as a reinforcing material in granular soil (sand) with varying degrees of compactness is a wonderful and advantageous design choice due to the significant improvement in bearing capacity at low settlement.

5.1.2 Influences of Reinforcement Layer Depth

It was well known that as reinforcement layer thickness declined, the building cost and time will significantly decline. If reinforcement of part from road base layer

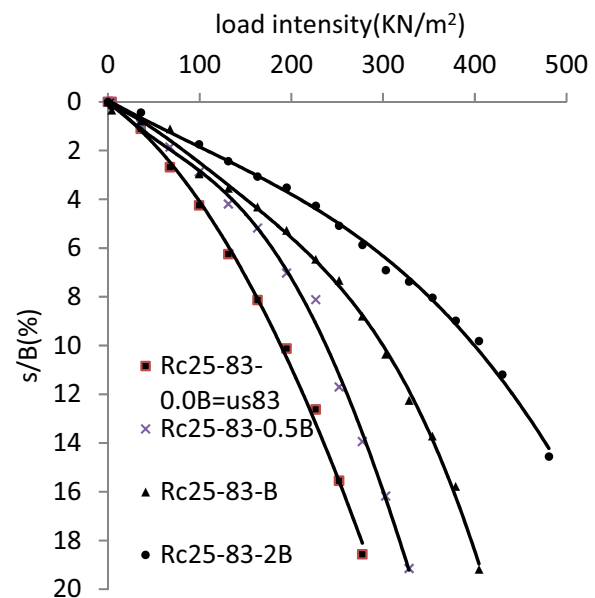


Fig. 12 Stress-settlement response of mixture incorporating 25% RC at different R_d (0B, 0.5B, B and 2B), Dr = 83%

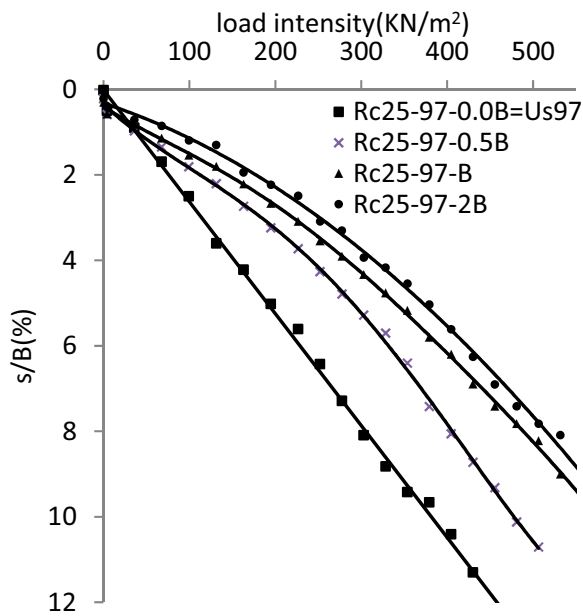


Fig. 13 Stress-settlement response of mixture incorporating 25% RC at different R_d (0B, 0.5B, B and 2B), $Dr=97\%$

will give same enhance in BCR of the mixture, reinforcement of complete thickness of road base layer is no requisite. As a result, reinforcement layer thickness was varied from 0 to 2B to investigate this aim. Figs. 12 and 13 show stress-settlement curves of mixture incorporating 25% RC at different reinforcement layer thickness

(R_d) 0B, 0.5B, B and 2B at $Dr=83\%$ and 97% , respectively. As expected, stress-settlement behavior (at $Dr=83\%$ and 97%) clearly improved with increase of R_d . In other words, energy capacity of mixture notably increased as R_d increased. This occurred due to increase of the strong reinforced layers beneath the footing model resisted more compressive stresses compared to unreinforced mixtures (US83 and US97). Additionally, as thickness of these strong reinforced layers increased, the soil mixture resisted high carry load capacity at small strains. It was shown that pressure-settlement behavior of the mixtures with $Dr=97\%$ were higher linear more than those of the mixtures with $Dr=83\%$ proving that as compaction degree increased, the behavior more improved.

To determine whether the impact of R_d on BCR of the mixture reinforced with 25% RC and compacted at two Dr 83 and 97% is beneficial, BCR change with s/B (%) at different R_d for $Dr=83\%$ and 97% is drawn in Figs. 14 and 15. The BCR of the mixtures were estimated in comparison to control specimens US83 and US97 with no reinforcement layer thickness. As seen in Figs. 12 and 13, BCR obviously enhanced when R_d increased from 0 to 2B at all s/B levels. It is should reported BCR of mixture RC25-83 which was 2.2, 2, 2, 2.06, and 2.05 at $s/B=2, 4, 6, 8$ and 10% (Sect. 5.1.1.1). This mixture was reinforced with 25% RC at full depth of the tank (4B) so we can refer this sample by RC25-83-4B. It was clear that maximum ratio of BCR was 120%. To evaluate the increase ratio in BCR resulting from variation of reinforcement layer thickness, we should consider this sample RC25-83-4B.

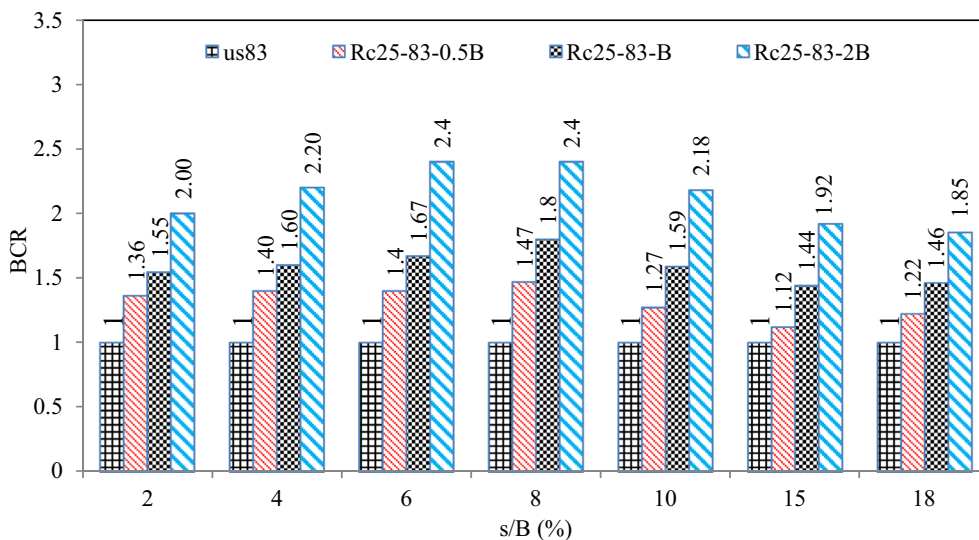


Fig. 14 BCR change with s/B at different R_d for $Dr=83\%$

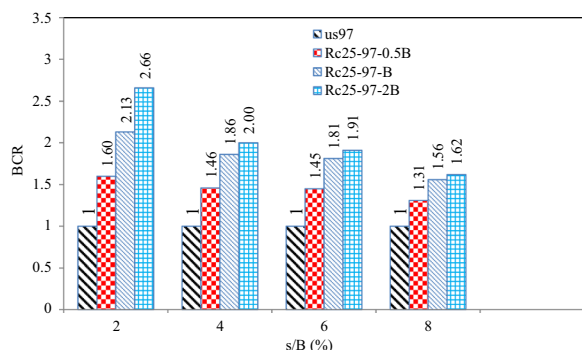


Fig. 15 BCR change with s/B at different R_d for $D_r = 97\%$

At $D_r = 83\%$, BCR obtained at $s/B = 2\%$ for R_d 0.5B, 1B, 2B and 4B was 1.36, 1.55, 2 and 2.2 while BCR obtained at $s/B = 4\%$ for R_d 0.5B, 1B, 2B and 4B was 1.4, 1.6, 2.2 and 2 proving that development in BCR slightly increased as strain (s/B) increased up to $s/B = 8\%$ then enhancement in BCR declined at high levels of strains. The maximum increase in BCR of mixture with $D_r = 83\%$ was 140% higher than that of US83 which occurred at $s/B = 8\%$ while the least increase in BCR was 12% larger that of US83 which took placed at $s/B = 15\%$. On the other hand, At $D_r = 97\%$, BCR remarked at $s/B = 2\%$ for R_d 0.5B, 1B and 2B was 1.6, 2.13 and 2.66 while BCR obtained at $s/B = 4\%$ for R_d 0.5B, 1B and 2B was 1.46, 1.86 and 2. BCR obtained at $s/B = 6\%$ for R_d 0.5B, 1B and 2B was 1.45, 1.81 and 1.91 while BCR obtained at $s/B = 8\%$ for R_d 0.5B, 1B and 2B was 1.31, 1.56 and 1.62. Showing that development in BCR slightly decreased as strain (s/B). For this reason, it was seen that performing partially reinforcing using RC caused better enhance in BCR at small strain at high density ($D_r = 97\%$). The maximum increase in BCR of mixture with $D_r = 97\%$ was 166% higher than that of US97 which occurred at $s/B = 2\%$ while the least increase in BCR was 31% larger that of US97 which took placed at $s/B = 8\%$. So that, effect R_d on improving BCR in density 97% was higher than that of density 83%. As listed in Sect. 5.1.1.2, BCR of mixture RC25-97 (may be referred as RC25-97-4B) was 2, 1.8, 1.67, 1.46, and 1.58 at $s/B = 2, 4, 6, 8$ and 10%. Showing that maximum increase in BCR was 100% at $s/B = 2\%$ when full tank was reinforced. When R_d equal 2B only (RC25-97-2B), increase in BCR was 160%. As a result, it is recommended the optimum thickness of reinforcement layer not exceed 2B either $D_r = 83\%$ or $D_r = 97\%$. This result will save cost and time of road base layer construction.

5.1.3 Influences of Relative Intensity

It is well known that as density of the mixture increased, effect of RC on strength and behavior of the soil will be higher but the cost and time of construction will increase due to high required quantity of water, soil and compaction. Therefore, enhancement in BCR of mixture due to increase in D_r from 83 to 97 is studied in this section. For achieving this goal, effect of D_r on stress-settlement response at different RC content (0, 25 and 50%) is drawn in Fig. 16 and effect of D_r on stress-settlement response of mixture incorporating 25% RC at different R_d (0.5B, 1B, 2B) is drawn in Fig. 17. In general, on stress-settlement response of mixture with $D_r = 97\%$ was better than that of mixture with $D_r = 83\%$ at all previous six cases drawn in Figs. 16 and 17 but with different degrees. As RC content within the sand increased, the difference between two curves of density 83% and 97% significantly declined. When RC reached 50%, two curves are similar approximately while two curves of mixtures with no RC are very varied. So, it is recommended that the relative density of 83% is enough acceptable at RC=50% and achieved same behavior of the relative density 97%. As shown in Fig. 17, as R_d increased, the difference in two curves declined. So, effect of D_r on stress-settlement response of mixture decreased with increase of reinforcement layer thickness.

Fig. 18 shows impact D_r on BCR at different RC content (0, 25 and 50%). The mixture with $D_r = 83\%$ is considered as a control specimen. It was noticed that enhancement in BCR due to increase of density from 83 to 97% decreased as RC increased where maximum increase in BCR was 100% at RC=0%, 61% at RC=25% and 17% at RC=50%. So, it is recommended that the relative density of 83% is enough acceptable at RC=50% and achieved same BCR of the relative density 97%. Table 3 listed increase ratios in BCR due to increase D_r from 83 to 97% at different s/B and RC. It is clear that all BCR values of $D_r = 83\%$ for two mixtures containing 25 and 50% RC are greater than the corresponding ones of $D_r = 97\%$. This is because of weak soils ($D_r = 83\%$) respond to improvement in BCR better than strong soils ($D_r = 97\%$) at all s/B values. The percentages of increase in BCR ranged from 20 to 327%. The best percentage of increase occurred in the mixture incorporating 50% RC at $s/B = 10\%$. The lowest percentage of increase occurred at $s/B = 2\%$ in the mixture incorporating 25% RC.

Fig. 19 shows relative density on BCR of mixture incorporating 25% RC at different R_d (0.5B, 1B, 2B). The mixture with $D_r = 83\%$ is considered as a referenced sample.

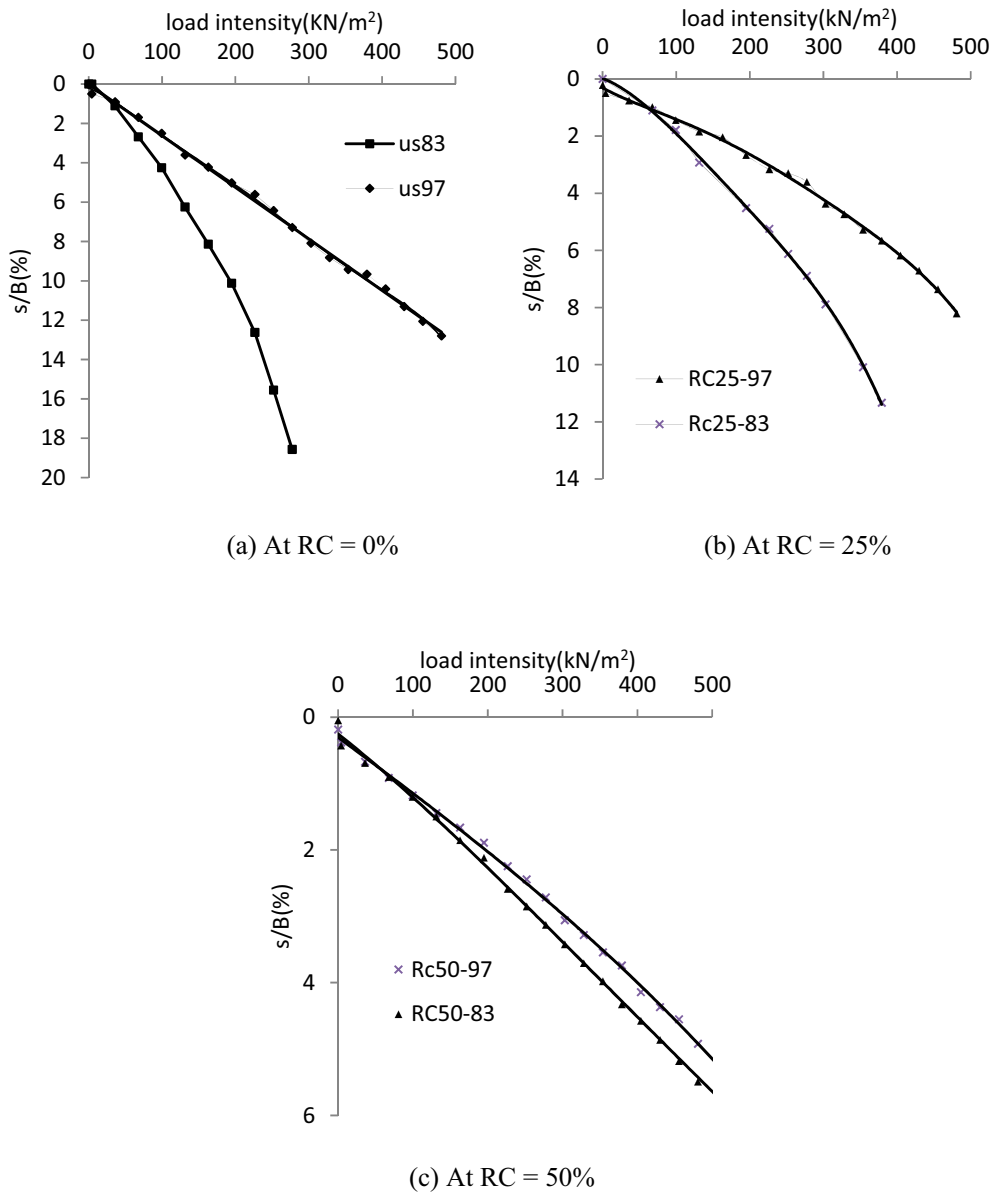


Fig. 16 Effect of D_r on stress-settlement response at different RC content (0, 25 and 50%)

It was noticed that enhancement in BCR due to increase of density from 83 to 97% declined as R_d increased from 0.5B to 2B where largest enhance in BCR was 122% at $R_d=0B$, 94% at $R_d=B$ and 91% at $RC=2B$. So, effect of D_r on BCR of mixture slightly declined with increase of reinforcement layer thickness. The reason is the pure sand under the reinforced layers is weak and the R_d should increase over 2B to decrease the difference between two relative densities.

5.2 Elasticity Modulus and Ultimate Bearing Capacity

5.2.1 Estimating Approach

Elasticity modulus (E) and ultimate bearing capacity (q_u) are important in the design and determining the E and q_u are essential. For this aim, stress-settlement curve of each tested mixture was used to find and hence estimate the E and q_u . The estimating approach used is illustrated as followed: (1) Drawing stress-strain diagram of each sample (Fig. 20) which is stress-settlement curve in the current work. (2) Performing

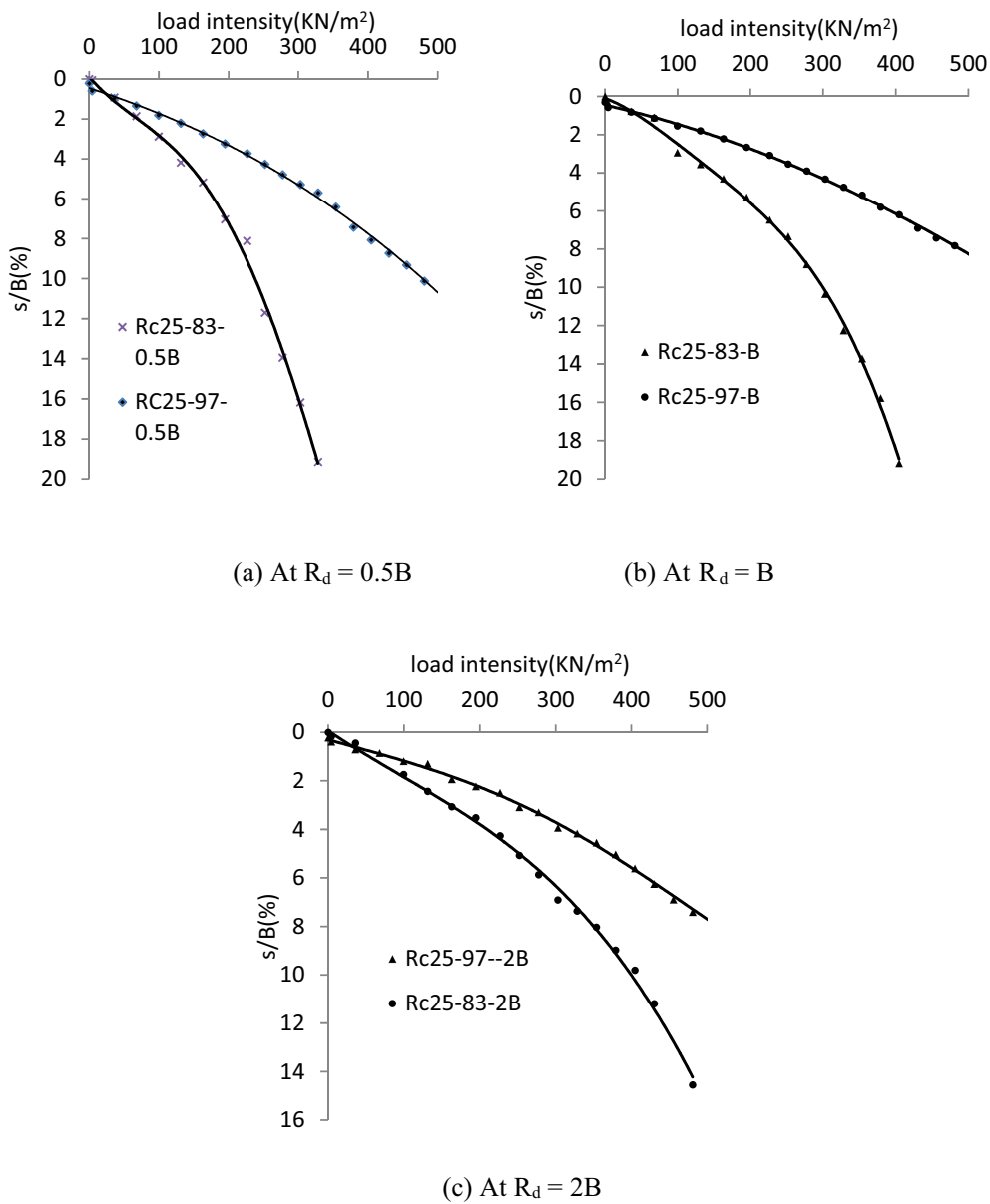


Fig. 17 Effect of D_r on stress-settlement response of mixture incorporating 25% RC at different R_d (0.5B, 1B, 2B)

two tangents of the curve where the initial tangent pass through the origin point and the other tangent pass through the end point. (3) Ultimate bearing capacity (q_u) is obtained at the intersection of two tangents. (4) Using Eq. (5) The bearing capacity of soil is defined as the capacity of the soil to bear the loads coming from the foundation. The pressure which the soil can easily withstand against load is called allowable bearing pressure. The bearing capacity of soil is defined as the

capacity of the soil to bear the loads coming from the foundation. The pressure which the soil can easily withstand against load is called allowable bearing pressure., to find allowable bearing capacity (q_a) according to ECP 202 (Basha, 2021) hence determine the corresponding allowable settlement (s_a). (5) Calculation of subgrade reaction modulus (k_s) using Eq. (6) (Bowles, 1997). 6) Using Eq. (7), the E could be estimated (Bowles, 1997).

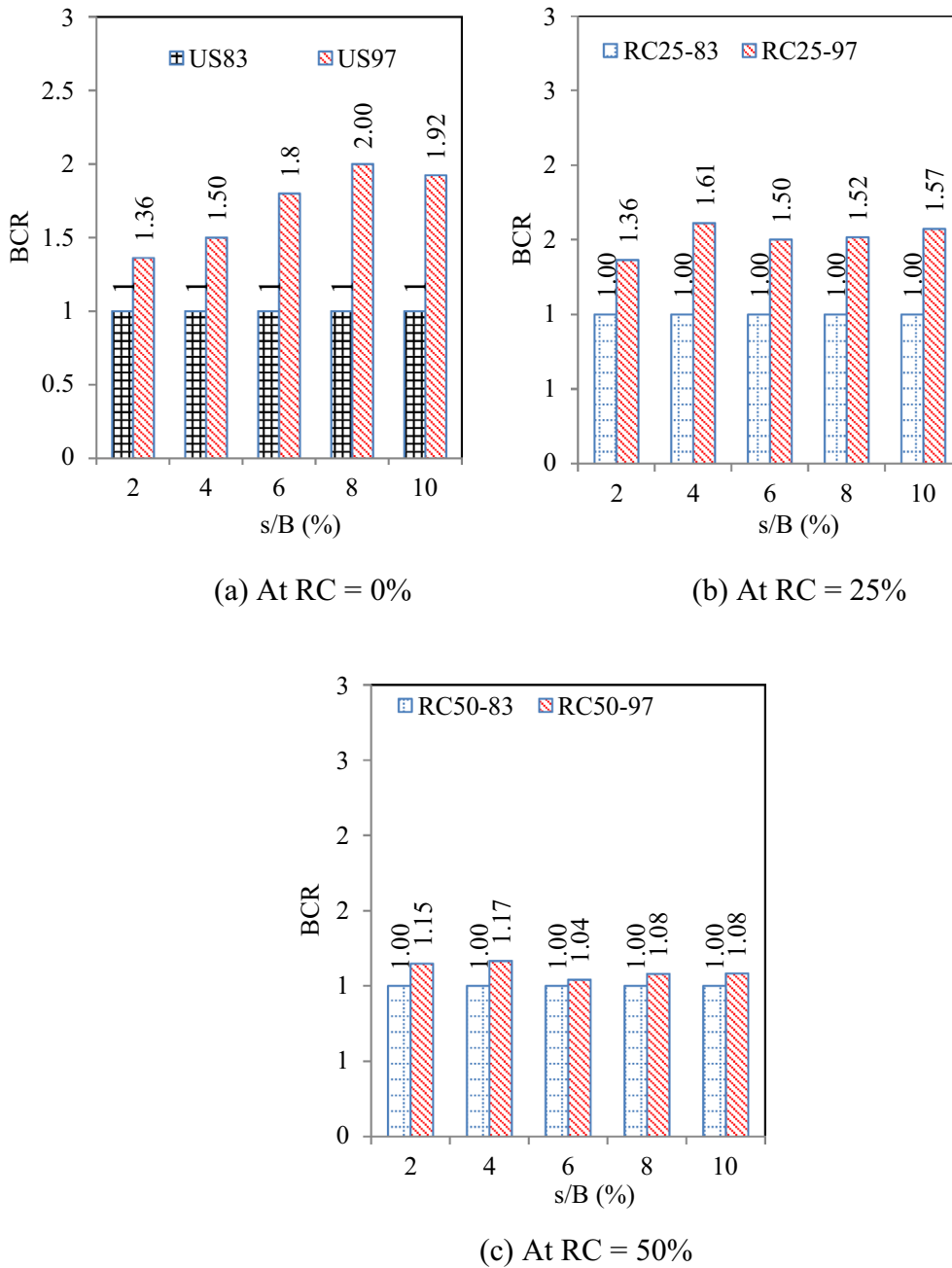


Fig. 18 Effect of Dr on BCR at different RC content (0, 25 and 50%)

$$q_a = \frac{q_u}{\text{factor}} \tag{5}$$

$$k_s = \frac{q_a}{s_a} \tag{6}$$

where factor is estimated 3 (Basha, 2021).

$$k_s = 1.13 \frac{E}{1 - \nu^2} * \frac{1}{\sqrt{A}} \tag{7}$$

Table 3 Values of increase ratio in BCR due to Dr at different s/B

| RC (%) | s/B (%) | BCR at Dr=83% | BCR at Dr=97% | Increase in BCR (%) |
|--------|---------|---------------|---------------|---------------------|
| 25 | 2 | 2.2 | 2 | 20 |
| | 4 | 2 | 1.8 | 20 |
| | 6 | 2 | 1.67 | 33 |
| | 8 | 2.06 | 1.56 | 50 |
| | 10 | 2.05 | 1.54 | 51 |
| 50 | 2 | 4.6 | 2.67 | 193 |
| | 4 | 4 | 2.26 | 174 |
| | 6 | 3.84 | 2.22 | 162 |
| | 8 | 3.7 | 1.87 | 183 |
| | 10 | 5 | 1.73 | 327 |

where A is the plate area (25×25 cm), ν is poisson ratio which was taken to be 0.33 according to (Rolfe et al., 2018).

The bearing capacity of soil is defined as the capacity of the soil to bear the loads coming from the foundation. The pressure which the soil can easily withstand against load is called allowable bearing pressure where q_u is The gross pressure at the base of the foundation at which soil fails is called ultimate bearing capacity where q_s is defined as B By considering only shear failure, net ultimate bearing capacity is divided by certain factor of safety will give the net safe bearing capacity Where F =factor of safety=3 (usual value) according to ECP 202 (Basha, 2021). Table 4 lists the results of the q_u and E of all tested samples.

5.2.2 Effect of RC

Fig. 21 shows effect of RC content on the q_u at Dr=83% and 97%. It was noticed that as RC increased, the the q_u increased. Increasing rate in the q_u was higher when Dr=83%. Relationship of the q_u -RC content was used to propose a new formula for estimating the q_u considering effect of RC content at two densities as below:

$$q_u = -0.0028 (RC)^3 + 0.268 (RC)^2 + 2.0737 (RC) + 274.4 \text{ at Dr} = 83\% \tag{8}$$

$$q_u = 0.176 (RC)^2 - 2 (RC) + 400 \text{ at Dr} = 97\% \tag{9}$$

Coefficient of determination (R^2) of Eq. (8) and (9) are 0.9965 and 1 proving good accuracy of these equations.

Fig. 22 shows effect of RC content on E at Dr=83% and 97%. It was noticed that as RC increased, the E improved. Relationship of E-RC content was used to propose a new formula for estimating E considering effect of RC content at two densities as below:

$$E = -0.1367 (RC)^3 + 9.9648 (RC)^2 - 26.619 (RC) + 1569.1 \text{ at Dr} = 83\% \tag{10}$$

$$E = -1.1888 (RC)^2 + 191.55 (RC) + 2000 \text{ at Dr} = 97\% \tag{11}$$

R^2 of Eq. (10) and (11) are 0.9956 and 1 proving good accuracy of these equations. These Eqs. (8–11) are useful and important for structural designers and future additional investigations in this field.

5.2.3 Effect of R_d

To more applicable, normalized depth of the reinforcement layer is used. This value was considered as dividing R_d by footing model dimension (B). Fig. 23 shows effect of R_d/B on the q_u at Dr=83% and 97%. It was noticed that as R_d increased, the the q_u increased. A proposed formulas were derived for estimating the q_u considering effect of R_d at two densities as below:

$$q_u = -9.0819 (R_d / B)^2 + 82.963 (R_d / B) + 256.15 \text{ at Dr} = 83\% \& RC = 25\% \tag{12}$$

$$q_u = -7.0571 (R_d / B)^2 + 45.41 (R_d / B) + 393.08 \text{ at Dr} = 97\% \& RC = 25\% \tag{13}$$

R^2 of Eq. (12) and (13) are 0.9671 and 0.9151 proving good accuracy of these equations.

Fig. 24 shows effect of R_d/B ratio on E at Dr=83% and 97%. It was noticed that as R_d/B increased, the E improved. Relationship of E- R_d/B was used to propose a new formula for estimating E considering effect of R_d at two densities as below:

$$E = -80.466 (R_d / B)^2 + 1294.4 (R_d / B) + 1045.4 \text{ at Dr} = 83\% \& RC = 25\% \tag{14}$$

$$E = -459.29 (R_d / B)^2 + 2986 (R_d / B) + 1522.1 \text{ at Dr} = 97\% \& RC = 25\% \tag{15}$$

R^2 of Eq. (14) and (15) are 0.9046 and 0.9452 proving good accuracy of these equations.

6 Predictive Models

The results of this research were subjected to linear multiple regressions in order to derive new formulas that could estimate the BCR, q_u , and E for all investigated

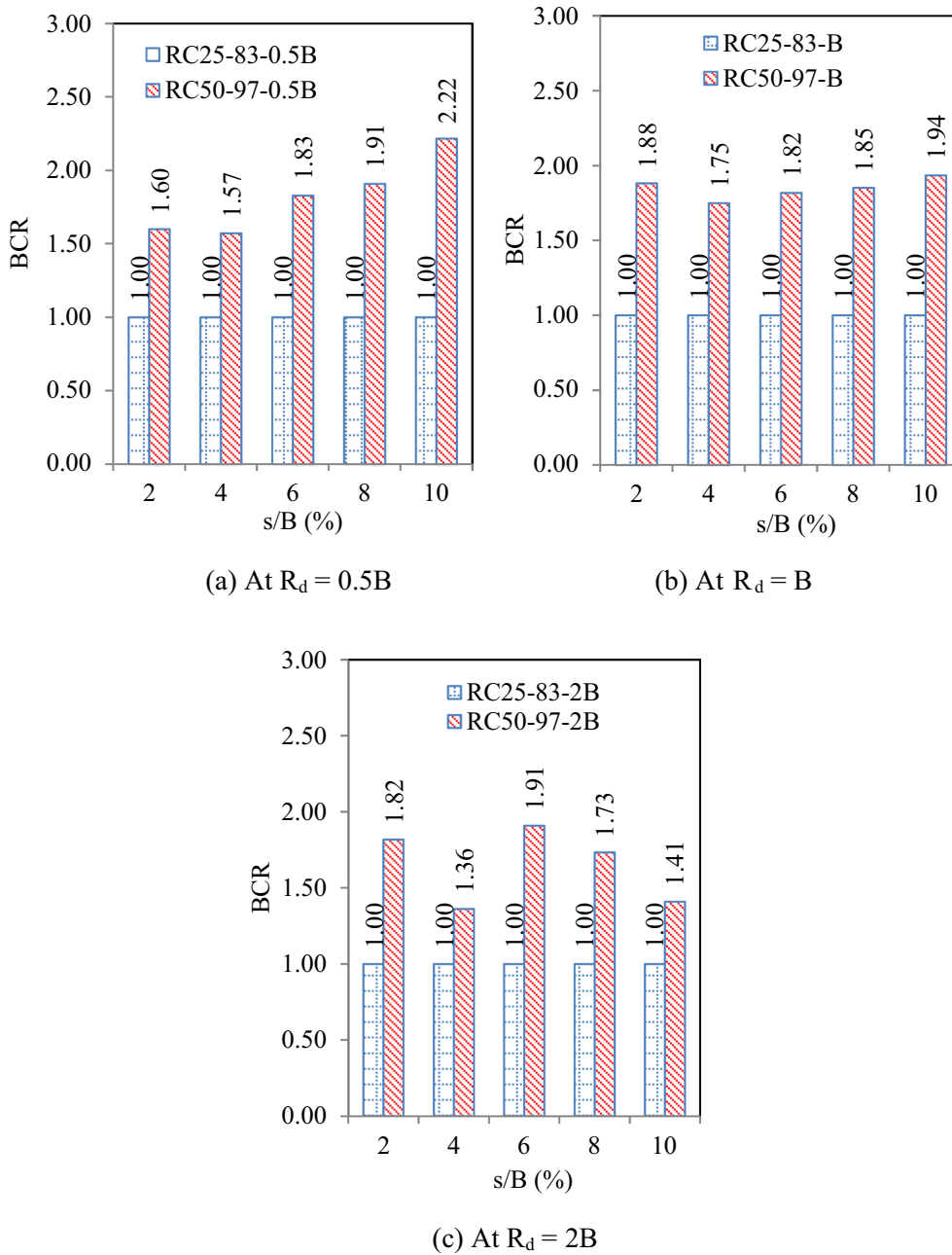


Fig. 19 Effect of D_r on BCR of mixture incorporating 25% RC at different R_d (0.5B, 1B, 2B)

mixes. It was investigated using Excel data analytics. The input variables taken into consideration for the current analysis are the RC %, s/B , R_d/B , and D_r . q_u , E , and BCR were chosen as the output parameters. There were 324 different input data sets in all. To get the best possible fit between the input and output parameters, many models

were tested. The best equations for forecasting the q_u , E , and BCR, respectively, are (16), (17), and (18):

$$q_u = -280.1 - 1.117 (s/B) + 6.651 (RC) + 5.448 (D_r) + 29.127 (R_d/B) \tag{16}$$

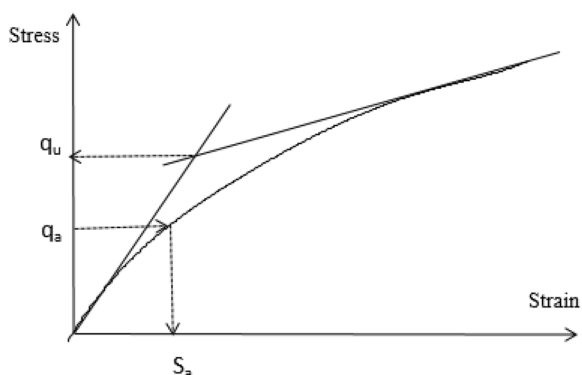


Fig. 20 Typical stress–strain diagram

Table 4 Results of the q_u and E of all tested samples

| Sample ID | RC (%) | R_d/B | q_u (kN/m ²) | E (kN/m ²) |
|--|--------|---------|----------------------------|--------------------------|
| Effect of RC at $Dr=83\%$ | | | | |
| US83 | 0 | 4 | 270 | 1432.2 |
| RC005-83 | 5 | 4 | 300 | 1798.4 |
| RC10-83 | 10 | 4 | 320 | 2294.24 |
| RC15-83 | 15 | 4 | 350 | 3094.92 |
| RC20-83 | 20 | 4 | 400 | 3650.85 |
| RC25-83 | 25 | 4 | 440 | 4833.39 |
| RC30-83 | 30 | 4 | 520 | 6107.51 |
| RC40-83 | 40 | 4 | 600 | 7885.84 |
| RC50-83 | 50 | 4 | 700 | 7986.78 |
| Effect of RC at $Dr=97\%$ | | | | |
| US97 | 0 | 4 | 400 | 2000 |
| RC25-83 | 25 | 4 | 460 | 6045.81 |
| RC50-83 | 50 | 4 | 740 | 8605.564 |
| Effect of R_d at $Dr=83\%$ & $RC=25\%$ | | | | |
| US83 | 25 | 0 | 270 | 1432.2 |
| RC25-83-0.5B | 25 | 0.5 | 280 | 1460 |
| RC25-83-B | 25 | 1 | 320 | 1600 |
| RC25-83-2B | 25 | 2 | 400 | 3900 |
| RC25-83 | 25 | 4 | 440 | 4833.39 |
| Effect of R_d at $Dr=97\%$ & $RC=25\%$ | | | | |
| US97 | 25 | 0 | 400 | 2000 |
| RC25-97-0.5B | 25 | 0.5 | 410 | 2200 |
| RC25-97-B | 25 | 1 | 420 | 4000 |
| RC25-97-2B | 25 | 2 | 466 | 6000 |
| RC25-97 | 25 | 4 | 460 | 6045.81 |

$$E = - 6270.417 - 18.533 (s / B) + 120.315 (RC) + 68.766 (Dr) + 578.766 (R_d / B) \tag{17}$$

$$BCR = 3.22 - 4.65e^{-02} (s / B) + 0.03867 (RC) - 2.5438e^{-02} (Dr) + 8.1616e^{-02} (R_d / B) \tag{18}$$

R^2 values of 0.87, 0.83, and 0.728 for Eqs. (16), (17), and (18) correspondingly showed good agreement. A correlation between experimental and anticipated values of ultimate bearing capacity, elasticity modulus, and BCR is shown in Figs. 25, 26, 27. The Eqs. (16–18) can be used with confidence to forecast the ultimate bearing capacity, elasticity modulus, and BCR of recycled concrete reinforced sandy soil since they are accurate for a wide variety of input variables, including $s/B=2-10\%$, $Dr=83\%$ and 97% , $RC=0$ to 50% , and $R_d/B=0$ to 4 .

To know and determine weight of each variable of the four studied parameter (s/B , Dr , RC and R_d/B) on q_u , E and BCR , standardized coefficients are shown in Fig. 28. From the data, it is clear that the recycled concrete (RC content) is the largest variable affecting q_u , E and BCR , followed by the R_d and then Dr . On contrast, s/B does not affect the q_u and E .

7 Application of RC-Sand Soil

The following list of applications for reinforced soils made from recycled concrete waste is provided: (1) For low volume rural roads, the high strengths and low strains of the RC-sandy soil mixture may have a financial impact. (2) Specific fill materials wouldn't be required thanks to the stability of the sandy soil. (3) Replacing poor soils and thickening the base layer in the subbases and subgrades of roads and pavement. (4) Replacement layer underneath shallow foundations to decrease the foundation depth, reduce settlement and increasinf the bearing capcity (5) Sandy soil that has been minimally stabilised and changed by cement can be substituted with RC-sandy soil combinations. (6) Backfilling for retaining walls and landfill liners are two more uses for RC-sandy mixtures. (7) Better strength outcomes are seen at very strains with higher RC concentration (small settlements recommended by design codes).

8 Conclusion

The effectiveness of recycled concrete aggregate (RC) in improving the structural performance of sandy soil is the main topic of this work, which focuses on a facility employing it to build road base layers. In order to accomplish this, two compaction levels for varying relative soil density ($Dr=83$ and 97%), RC contents ($0,5,10,15,20,25,30,40,50$ and 100%), and different thickness of the reinforcement layer ($R_d=0.0B, 0.5B, B,$ and $2B$ where B is the footing model dimension) were carried out. In order to investigate the effects of key factors on

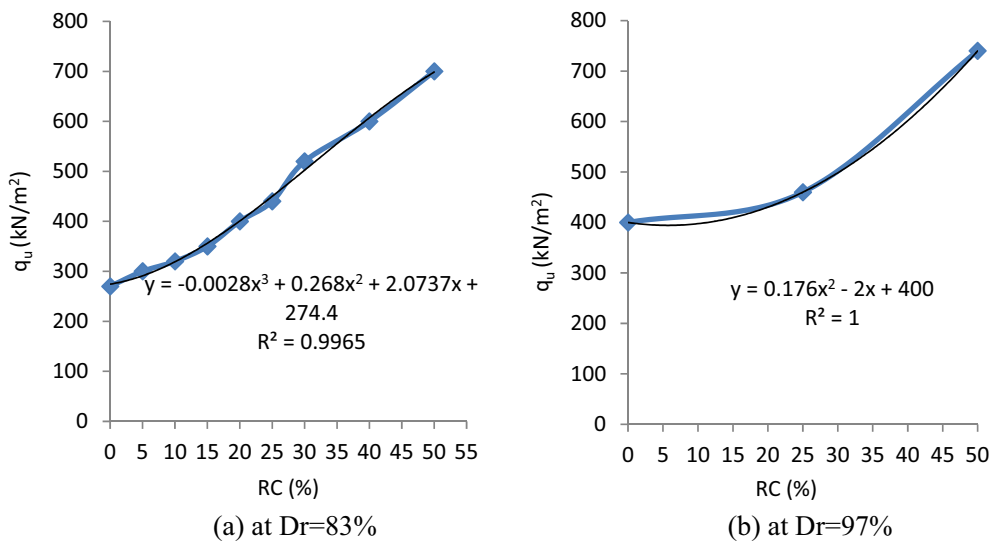


Fig. 21 Effect of RC content on the q_u

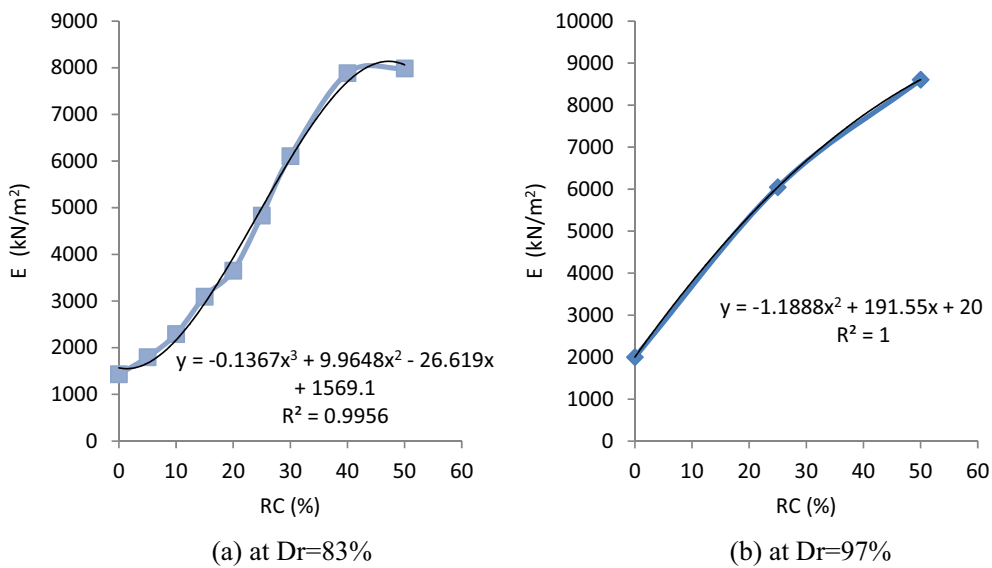
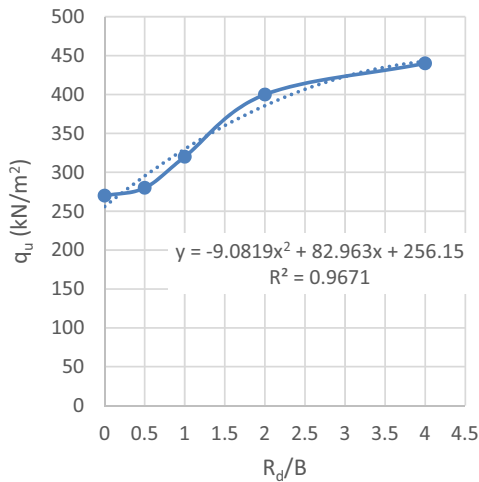


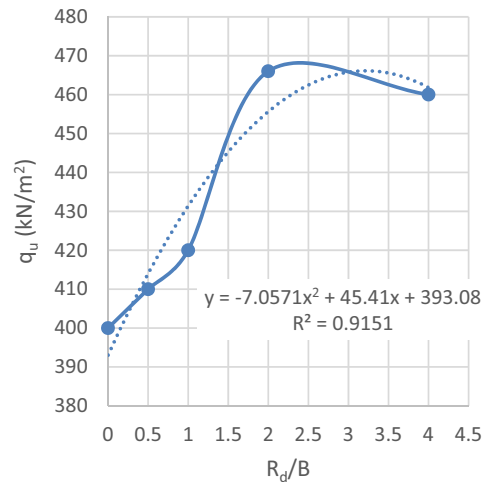
Fig. 22 Effect of RC content on E

the properties of the mixtures, such as grain size distribution, effective/average grain sizes, uniformity/curvature coefficients, bulk density/specific gravity, maximum dry density, and ideal water content, numerous laboratory experiments were carried out. The plate bearing experiments were performed using a footing model

(250×250 mm) inside a tank (1500×1500×1000 mm) to ascertain the stress–strain response, bearing capacity ratio (BCR), ultimate bearing capacity, and modulus of elasticity of the tested mixtures. The results showed the following findings:

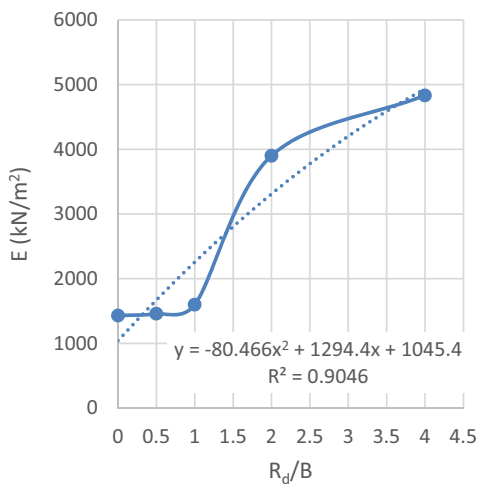


(a) at Dr=83%

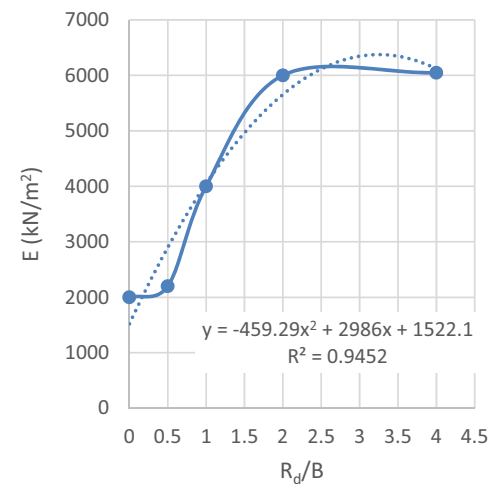


(b) at Dr=97%

Fig. 23 Effect of R_d on the q_u & RC=25%



(a) at Dr=83%



(b) at Dr=97%

Fig. 24 Effect of R_d/B on E & RC=25%

- 1) The method utilised to mix the RC with the sand is an excellent one and is appropriate for usage in the field. It is evident that increasing the RC up to 40% has no impact on grain size diameters, while increasing it to 50% has a minimal impact. The rate of increase in diameters is fairly rapid when the RC exceeds 50%.
- 2) When RC grew from 0 to 50%, the uniformity coefficient gradually increased. However, when RC hit 100%, it was evidently higher because there were no

longer any fine sand particles. Contrarily, because it is inversely related to the diameter mean diameter, which climbed as RC rose, curvature coefficient decreased as RC increased.

- 3) It was observed that the bulk density of the mixture grew as RC increased up to 50%. Because there were no fine sand particles in in completely RC mixture, bulk density declined at RC increased more than 50%.

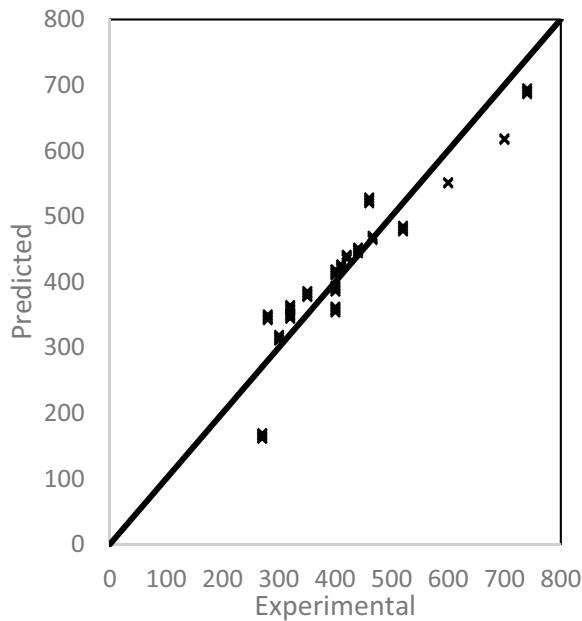


Fig. 25 Experimental versus predicted values of ultimate bearing capacity (q_u)

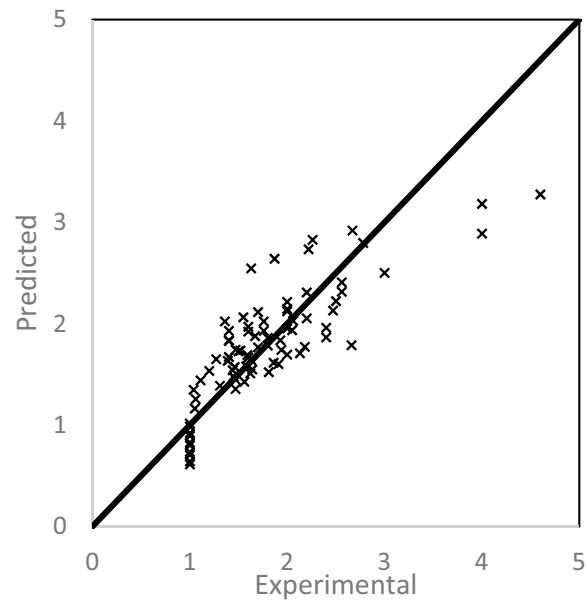


Fig. 27 Experimental versus predicted values of bearing capacity ratio (BCR)

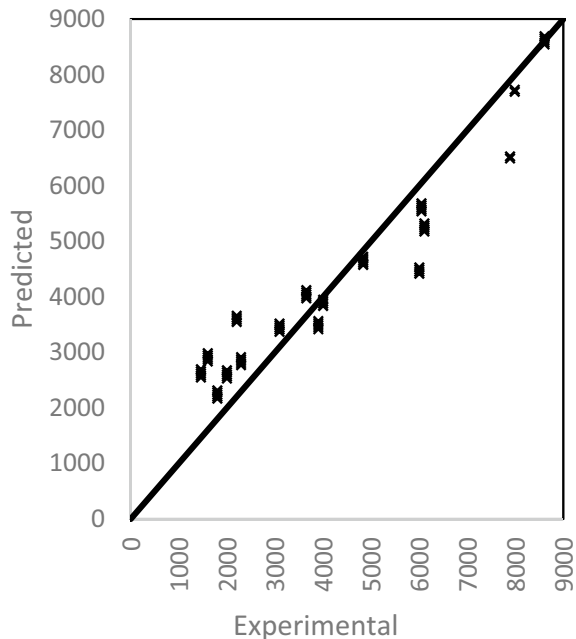


Fig. 26 Experimental versus predicted values of elasticity modulus (E)

4) The pressure-settlement relationship was greatly improved by utilising RC as a reinforcement material inside the soil. Additionally, the soil developed a stronger relationship between pressure and settlement as RC grew.

- 5) It was observed that for all RC levels (0–50%) and all values of settlement ratio (2–12%), BCR definitely rose as RC increased. It was shown that at extremely small strains (settlement ratio=2%), the increase in BCR was greatest. As a result of the significant improvement in bearing capacity at low settlement, using RC as a reinforcing material in granular soil (sand) is a fantastic and advantageous design decision.
- 6) Pressure-settlement behavior (at $D_r=83\%$ and 97%) clearly improved with increase of R_d . moreover, BCR obviously enhanced when R_d increased from 0 to $2B$ at all settlement ratios. Therefore, it is advised that the ideal reinforcing layer thickness not exceed $2B$ either $D_r=83\%$ or $D_r=97\%$. The construction of the road's subbase will be faster and cheaper as a result.
- 7) It is recommended that the relative density of 83% is enough acceptable at $RC=50\%$ and achieved same behavior of the relative density 97%.
- 8) The difference between two pressure-settlement curves of densities 83% and 97% significantly diminished as reinforcement layer thickness rose. Therefore, as the thickness of the reinforcing layer increased, the effect of D_r on the mixture's pressure-settlement response reduced. It was observed that ultimate bearing capacity and elasticity modulus of the tested mixtures rose as RC and R_d increased. When $D_r=83\%$, the increasing rate was higher than that of $D_r=97\%$.

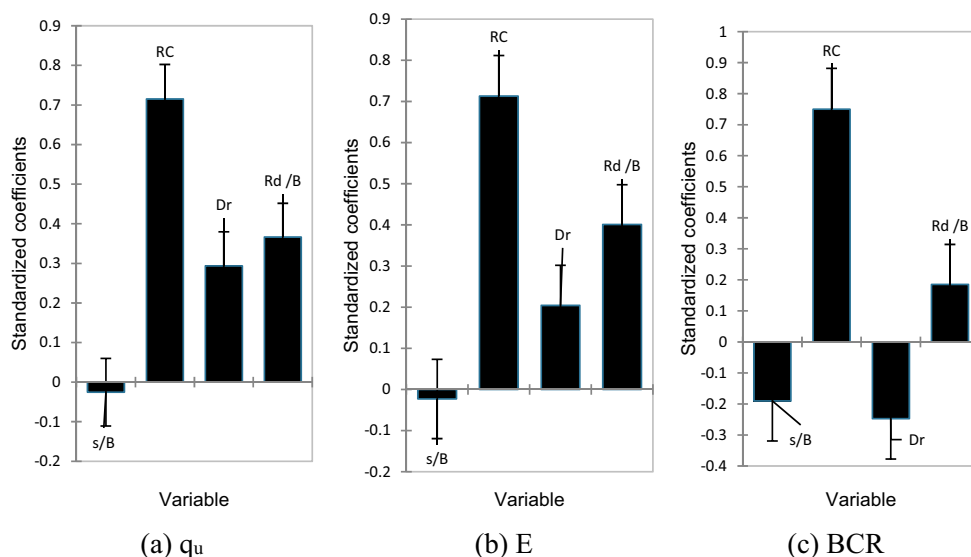


Fig. 28 Weights of standardized coefficients

List of symbols

| | |
|-----------------|--|
| B | Footing model width |
| Cc | Coefficient of curvature |
| Cu | Uniformity coefficient |
| D ₁₀ | Effective grain size |
| D ₅₀ | Average grain size |
| Dr | Relative density of the mixture |
| E | Elasticity modulus |
| G _s | Specific gravity |
| k _s | Subgrade reaction modulus |
| M _{RC} | Mass of the recycled concrete (RC) |
| M _{US} | Mass of the unreinforced sand (US) |
| q _a | Allowable bearing capacity |
| q _u | Ultimate bearing capacity |
| R _d | Reinforcement depth |
| s | Settlement |
| s/B | Settlement ratio |
| s _a | Allowable settlement |
| V | Is volume of the one layer of the tank |
| v | Poison ratio |
| ρ | Density of the mixture |
| US | Unreinforced sand |
| RC | Recycled concrete |
| BD | Bulk density |
| MDD | Maximum dry density |
| OMC | Optimum water content |
| BCR | Bearing capacity ratio |
| RCA | Recycled concrete aggregate |

Acknowledgements

The tests were carried out in the soil Laboratory, Faculty of Engineering, kafrElshiekh University, Egypt. The present work is an extension of the Master of Science thesis of the second author.

Author contributions

AB: Resources, investigation, data curation, writing-original draft, reviewing. FK: investigation, data curation, validation, writing-original draft, visualization, writing—review & editing. SF: investigation, data curation, writing—original draft, visualization, writing—review & editing. All authors read and approved the final manuscript.

Funding

Open access funding provided by The Science, Technology & Innovation Funding Authority (STDF) in cooperation with The Egyptian Knowledge Bank (EKB). No fund.

Availability of data and materials

The experimental data can be obtained through email communication with the author at sabry_fayed@eng.kfs.edu.eg.

Declarations

Ethics approval and consent to participate

Not applicable.

Informed consent

Informed consent was obtained from all individual participants included in this study.

Consent for publication

All the authors agree that the article will be published after acceptance.

Competing interests

The authors declare that they have no competing interests.

Author details

¹Civil Engineering Department, Faculty of Engineering, Kafrelshiekh University, Kafr El Sheikh, Egypt.

Received: 18 February 2023 Accepted: 6 May 2023

Published online: 09 October 2023

References

Al-Mukhtar, M., Lasledj, A., & Alcover, J.-F. (2010). Behaviour and mineralogy changes in lime-treated expansive soil at 20 C. *Applied Clay Science*, 50(2), 191–198.

Arabani, M., Nejad, F. M., & Azarhoosh, A. R. (2013a). Laboratory evaluation of recycled waste concrete into asphalt mixtures. *International Journal of Pavement Engineering*, 14.6, 531–539.

Arulrajah, A., Piratheepan, J., Disfani, M. M., & Bo, M. W. (2013). Geotechnical and geoenvironmental properties of recycled construction and demolition materials in pavement subbase applications. *Journal of Materials in*

- Civil Engineering*, 25(8), 1077–1088. [https://doi.org/10.1061/\(ASCE\)MT.1943-5533.0000652](https://doi.org/10.1061/(ASCE)MT.1943-5533.0000652)
- Askarian, M., Tao, Z., Adam, G., & Samali, B. (2018). Mechanical properties of ambient cured one-part hybrid OPC-geopolymer concrete. *Construction and Building Materials*, 186, 330–337.
- ASTM D2487. (2017). Standard Practice for Classification of Soils for Engineering Purposes, ASTM International, West Conshohocken, PA
- Ates, A. (2016). Mechanical properties of sandy soils reinforced with cement and randomly distributed glass fibers (GRC). *Composites Part B Engineering*, 96, 295–304.
- Basha, A. M. (2021). Post buckling behavior of slender piles partially embedded in sand soil under axial load. *KSCCE Journal of Civil Engineering*, 25(3), 757–767.
- Belmokhtar, N., Ammari, M., Brigui, J., & Ben allal, L. (2017). Comparison of the microstructure and the compressive strength of two geopolymers derived from Metakaolin and an industrial sludge. *Construction and Building Materials*, 146, 621–629.
- Blanck, G., Cuisinier, O., & Masroui, F. (2014). Soil treatment with organic non-traditional additives for the improvement of earthworks. *Acta Geotechnica*, 9(6), 1111–1122.
- Bowles, J. E. (1997). *Foundation analysis and design* (5th ed.). McGraw-Hill Inc.
- Cabalar, A. F., Abdulnafaa, M. D., & Isbuga, V. (2021). Plate loading tests on clay with construction and demolition materials. *Arabian Journal for Science and Engineering*, 46, 4307–4317.
- Caballero, E., Sanchez, W., & Rios, C. A. (2014). Synthesis of geopolymers from alkaline activation of gold mining wastes. *Ingenieria y Competitividad*, 16(1), 317–330.
- Cristelo, N., Glendinning, S., Fernandes, L., & Pinto, A. T. (2013). Effects of alkaline-activated fly ash and Portland cement on soft soil stabilisation. *Acta Geotechnica*, 8(4), 395–405.
- Davies, H. T., Nutley, S. M., & Smith, P. C. (1999). *Editorial: What works? The role of evidence in public sector policy and practice*. Bristol University Press.
- ECP-202. (2018). Egyptian Code of Practice for Soil Mechanics and Foundations Design and Construction, Housing and Building National Research Center, Ministry of Housing, Utilities and Urban Planning, Cairo
- Gálvez-Martos, J.-L., Styles, D., Schoenberger, H., & Zeschmar-Lahl, B. (2018). Construction and demolition waste best management practice in Europe. *Resources, Conservation and Recycling*, 136, 166–178.
- Geckil, T., Sarici, T., & Ok, B. (2022). Model studies on recycled whole rubber tyre reinforced granular fillings on weak soil. *Revista De La Construcción*, 21(2), 264–280. <https://doi.org/10.7764/rdlc.21.2.264>
- Gill, G., & Mittal, R. K. (2019). Use of waste tire-chips in shallow footings subjected to eccentric loading-an experimental study. *Construction and Building Materials*, 199, 335–348.
- Haider I, et al. (2014) Evaluation of the mechanical performance of recycled concrete aggregates used in highway base layers. Geo-Congress 2014: Geo-characterization and Modeling for Sustainability, pp. 3686–3694
- Harr, M. E. (1966). *Foundations of Theoretical Soil Mechanics*. National Academies Press.
- Horpibulsuk, S., Rachan, R., Chinkulkijniwat, A., Raksachon, Y., & Suddeepong, A. (2010). Analysis of strength development in cement-stabilized silty clay from microstructural considerations. *Construct Build Mater*, 24(10), 2011–2021.
- IS: 2720. (1983) Methods of test for soils – determination of density index for cohesionless soils, New Delhi, Bureau of Indian Standards, 1983.
- Islam, A., Alengaram, U. J., Jumaat, M. Z., & Bashar, I. I. (2014). The development of compressive strength of ground granulated blast furnace slag-palm oil fuel ash-fly ash based geopolymer mortar. *Materials and Design*, 56, 833–841.
- Jiménez, J. R., Ayuso, J., Agrela, F., López, M., & Galvin, A. P. (2012). Utilisation of unbound recycled aggregates from selected CDW in unpaved rural roads. *Resources, Conservation and Recycling*, 58, 88–97.
- Kim, M. S., Jun, Y., Lee, C., & Oh, J. E. (2013). Use of CaO as an activator for producing a price-competitive non-cement structural binder using ground granulated blast furnace slag. *Cement and Concrete Research*, 54, 208–214.
- Kim, Y., & Jeong, S. (2011). Analysis of soil resistance on laterally loaded piles based on 3d soil–pile interaction. *Computers and Geotechnics*, 38, 248–257.
- Ladd, R. S. (1978). Preparing test specimens using undercompaction. *Geotechnical Testing Journal*, 1, 16–23.
- Latifi, N., Eisazadeh, A., & Marto, A. (2014). Strength behavior and microstructural characteristics of tropical laterite soil treated with sodium silicate-based liquid stabilizer. *Environment and Earth Science*, 72(1), 91–98.
- Latifi, N., Meehan, C. L., Majid, M. Z. A., & Horpibulsuk, S. (2016). Strengthening montmorillonitic and kaolinitic clays using a calcium-based non-traditional additive: A micro-level study. *Applied Clay Science*, 132–133, 182–193.
- A. Lim, Y.A. Montol, S. Rustiani. (2021). Soil improvement using xanthan gum biopolymer for loose sand: experimental study, proceedings of the international conference on civil, offshore environ. Eng. (pp. 349–355). Springer
- Maghool, F., Arulrajah, A., Du, Y.-J., Horpibulsuk, S., & Chinkulkijniwat, A. (2017). Environmental impacts of utilizing waste steel slag aggregates as recycled road construction materials. *Clean Technologies and Environmental Policy*, 19(4), 949–958.
- Maragkos, I., Giannopoulou, I. P., & Panias, D. (2009). Synthesis of ferronickel slag-based geopolymers. *Minerals Engineering*, 22(2), 196–203.
- Mehrdadi, G. T., Azizi, A., Haji-Azizi, A., & Asdollahfardi, G. (2020). Evaluating and improving the construction and demolition waste technical properties to use in road construction. *Transportation Geotechnics*, 23, 100349. <https://doi.org/10.1016/j.trgeo.2020.100349>
- Mohammadinia, A., Arulrajah, A., Sanjayan, J., Disfani, M. M., Bo, M. W., & Darmawan, S. (2015). Laboratory evaluation of the use of cement-treated construction and demolition materials in pavement base and subbase applications. *J Mater Civil Eng*, 27(6), 04014186. [https://doi.org/10.1061/\(ASCE\)MT.1943-5533.0001148](https://doi.org/10.1061/(ASCE)MT.1943-5533.0001148)
- Mohammadinia, A., Arulrajah, A., D'Amico, A., & Horpibulsuk, S. (2018). Alkali-activation of fly ash and cement kiln dust mixtures for stabilization of demolition aggregates. *Construction and Building Materials*, 186, 71–78.
- Mohammadinia, A., Arulrajah, A., Horpibulsuk, S., & Tabatabaie Shourijeh, P. (2019). Impact of potassium cations on the light chemical stabilization of construction and demolition wastes. *Construction and Building Materials*, 203, 69–74.
- Ok, B., Sarici, T., Talaslioglu, T., & Yildiz, A. (2020). Geotechnical properties of recycled construction and demolition materials for filling applications. *Transp Geotech*, 24, 100380.
- Ok, B., Sarici, T., Demir, A., Talaslioglu, T., & Yildiz, A. (2023). Investigation of construction and demolition materials reinforced by geosynthetics. *Proceedings of the Institution of Civil Engineers - Engineering Sustainability*. <https://doi.org/10.1680/jensu.22.00077>
- Pan, Z., Tao, Z., Cao, Y.-F., & Wuhrer, R. (2018). Measurement and prediction of thermal properties of alkali-activated fly ash/slag binders at elevated temperatures. *Materials and Structures*, 51(4), 108.
- Pérez, I., Pasandín, A. R., & Medina, L. (2012). Hot mix asphalt using C&D waste as coarse aggregates. *Materials & Design*, 36, 840–846.
- Pourakbar, S., Asadi, A., Huat, B. B. K., & Fasihnikoutalab, M. H. (2015). Soil stabilization with alkali-activated agro-waste. *Environ Geotechn*, 2(6), 359–370.
- Rios, S., Ramos, C., da Fonseca, A. V., Cruz, N., & Rodrigues, C. (2016). Colombian soil stabilized with geopolymers for low cost roads. *Procedia Eng*, 143, 1392–1400.
- Rolfe, A., Huang, Y., Haaf, M., Pita, A., Rezvani, S., Dave, A., & Hewitt, N. J. (2018). Technical and environmental study of calcium carbonate looping versus oxy-fuel options for low CO₂ emission cement plants. *International Journal of Greenhouse Gas Control*, 75, 85–97.
- Rowles, M., & O'connor, B. (2003). Chemical optimisation of the compressive strength of aluminosilicate geopolymers synthesised by sodium silicate activation of metakaolinite. *Journal of Materials Chemistry*, 13(5), 1161–1165.
- Santa, R. A. B., Bernardin, A. M., Riella, H. G., & Kuhnen, N. C. (2013). Geopolymer synthesized from bottom coal ash and calcined paper sludge. *J Cleaner Prod*, 57, 302–307.
- Shen, W., Cao, L., Li, Q., Zhang, W., Wang, G., & Li, C. (2015). Quantifying CO₂ emissions from China's cement industry. *Renewable and Sustainable Energy Reviews*, 50, 1004–1012.
- Suksiripattanaopong, C., Kua, T.-A., Arulrajah, A., Maghool, F., & Horpibulsuk, S. (2017). Strength and microstructure properties of spent coffee grounds stabilized with rice husk ash and slag geopolymers. *Construction and Building Materials*, 146, 312–320.
- Vásquez, A., Cardenas, V., Robayo, R. A., & de Gutiérrez, R. M. (2016). Geopolymer based on concrete demolition waste. *Advanced Powder Technology*, 27(4), 1173–1179.

- Vieira, C. S., & Pereira, P. M. (2015). Use of recycled construction and demolition materials in geotechnical applications: A review. *Resources, Conservation and Recycling*, 103, 192–204.
- Yong, R., & Ouhadi, V. (2007). Experimental study on instability of bases on natural and lime/cement-stabilized clayey soils. *Applied Clay Science*, 35(3–4), 238–249.
- Zaetang, Y., et al. (2016). "Properties of pervious concrete containing recycled concrete block aggregate and recycled concrete aggregate. *Construction and Building Materials*, 111, 15–21.
- Zhang, G., He, J., & Gambrell, R. P. (2010). Synthesis, characterization, and mechanical properties of red mud-based geopolymers. *Transportation Research Record*, 2167(1), 1–9.
- Zhang, M., El-Korchi, T., Zhang, G., Liang, J., & Tao, M. (2014). Synthesis factors affecting mechanical properties, microstructure, and chemical composition of red mud-fly ash based geopolymers. *Fuel*, 134, 315–325.

Publisher's Note

Springer Nature remains neutral with regard to jurisdictional claims in published maps and institutional affiliations.

Ali Basha: Associate Professor, Department of Civil Engineering, Faculty of Engineering, Kafrelsheikh University, Kafrelsheikh, Egypt.

Fatma khalifa: Msc student, Civil Engineering Department, Faculty of Engineering, Kafrelshiekh University, Egypt.

Sabry Fayed: Associate Professor, Department of Civil Engineering, Faculty of Engineering, Kafrelsheikh University, Kafrelsheikh, Egypt.

Submit your manuscript to a SpringerOpen[®] journal and benefit from:

- Convenient online submission
- Rigorous peer review
- Open access: articles freely available online
- High visibility within the field
- Retaining the copyright to your article

Submit your next manuscript at ► [springeropen.com](https://www.springeropen.com)
